

1-1-2008

A dynamic CIP/CIL process simulation using MATLAB SIMULINK

Heino Deist

Cape Peninsula University of Technology

Recommended Citation

Deist, Heino, "A dynamic CIP/CIL process simulation using MATLAB SIMULINK" (2008). *CPUT Theses & Dissertations*. Paper 7.
http://dk.cput.ac.za/td_cput/7

This Text is brought to you for free and open access by the Theses & Dissertations at Digital Knowledge. It has been accepted for inclusion in CPUT Theses & Dissertations by an authorized administrator of Digital Knowledge. For more information, please contact barendsc@cput.ac.za.

A DYNAMIC CIP/CIL PROCESS SIMULATION USING MATLAB SIMULINK

BY

HEINO DEIST

A Thesis submitted in fulfillment of the requirements for the
Masters Degree in Technology
(Chemical Engineering)
at the Cape Peninsula University of Technology

SUPERVISOR: J.W. COETZEE

CPUT

2008

The Financial assistance of the Cape Peninsula University of Technology (CPUT) is hereby acknowledged. The opinions expressed and conclusions arrived at are not necessarily to be attributed to CPUT.

DECLARATION

I hereby certify that this thesis is my own original work, except where specifically acknowledged in the text

H.E. Deist

Date

ABSTRACT

Carbon-in-pulp (CIP) technology is firmly entrenched in the mining sector due to numerous advances in the last few decades. CIP technology recovers complexed gold in solution from slurry streams by contacting the pulp with carbon and separating the two by screening. The carbon-in-leach (CIL) process, where the pulp contains free cyanide, is closely related to CIP. Both these processes, especially CIL, are complex and are governed by a number of interacting unit processes. The overall process efficiency is dependant on a large number of variables, making the process difficult to optimize.

This study uses simple adsorption and leaching rate equations in order to predict dynamic CIL/CIP plant performance under varying operating conditions. This will assist plant metallurgists to achieve optimum efficiency, highlight plant sensitivity to certain variables and will ultimately result in proactive process control. Various assumptions were made in order to keep the modeling considerations as simple and realistic as possible. The process was assumed to have linear kinetic and equilibrium operation. The process was simulated using Simulink in Matlab. Variables are solved on a time step basis by Matlab's built in optimization algorithms.

Simulation results illustrated that the use of simple leaching and adsorption rate expressions are effective for investigating dynamic plant behavior under changing operating conditions.

ACKNOWLEDGEMENTS

The work contained in this thesis was performed at the Department of Chemical Engineering at the Cape Peninsula University of Technology (Cape Town Campus) between January and December 2005.

I thank the following individuals/institutions for their assistance and contributions towards the completion of this thesis:

- My supervisor and mentor, Mr. J.W. Coetzee for his advice, guidance and support.
- The Department of Chemical Engineering at the Cape Peninsula University of Technology (CT) for the use of their facilities and financial contribution to my work.
- AngloGold for the use of their plant data
- Fellow colleagues, students and friends, especially Mrs. M. van den Bosch, for their moral support, advice and uplifting conversation.
- My parents for their faith in me, their love and financial support.
- My God and savior, the greatest engineer of all. You are the reason I enjoy typing this section. Without appreciation I am nothing!

CONTENTS

	PAGE
DECLARATION.....	ii
ABSTRACT	iii
ACKNOWLEDGEMENTS	iv
CONTENTS	v
LIST OF TABLES.....	viii
LIST OF FIGURES	ix
NOMENCLATURE	xii
CHAPTER 1: INTRODUCTION.....	1
1.1. Background	1
1.2. Project Motivation	1
1.3. Objectives	3
1.4. Plan of Development	4
CHAPTER 2: LITERATURE REVIEW.....	5
2.1. The Carbon-in-Pulp Process	5
2.2. The Carbon-in-Leach Process	9
2.3. CIP/CIL Modelling Considerations	10
2.4. Adsorption Kinetics	12
2.5. Leaching Kinetics	13
2.6. Other Metals	15
2.7. Solution Methods of Matlab Simulink	16

CHAPTER 3: METHODOLOGY	20
3.1. Modelling Considerations	20
3.2. Mass Balances	24
3.2.1. Mass Balances for Gold and OM	25
3.2.2. Cyanide Consumption	27
3.2.3. Overall Gold Removal	27
3.3. Simulink Interface	28
3.3.1. Tank Example	36
3.4. Simulation Architecture	41
3.4.1. Stage Block	41
3.4.2. Gold And OM Sub-systems	45
3.4.3. Leaching Sub-system	48
3.4.4. Adsorption Sub-system	50
3.4.5. Carbon Loading Sub-system	52
3.4.6. Cyanide Consumption Sub-system	57
3.4.7. Overall Gold Removal Sub-system	59
CHAPTER 4: RESULTS FOR PARAMETER ESTIMATION	60
4.1. Modelling	60
CHAPTER 5: RESULTS FOR DYNAMIC CIP PLANT SIMULATION	63
5.1. Start-up Simulation (Unsteady)	65
5.2. Simulation Using Initial Carbon Loadings (Plant data)	72
CHAPTER 6: RESULTS FOR SENSITIVITY ANALYSIS	76
6.1. Step-change in Liquid Feed Gold Concentration	77
6.2. Step-change in Solids Feed Rate	85
6.3. Step-change in Elution Efficiency	91

CHAPTER 7: CONCLUSIONS	97
BIBLIOGRAPHY	99
APPENDIX A	101

LIST OF TABLES

	PAGE
<i>Table 4.1. : Actual Plant Data used for CIP Modelling</i>	60
<i>Table 4.2. : Plant Data Converted for Simulation Input.</i>	60
<i>Table 4.3. : Equivalent Discrete Carbon Flow Rate.</i>	61
<i>Table 4.4. : Stage-by-stage Adsorption Data.</i>	61
<i>Table 4.5. : Comparison of Plant data vs. Simulated data.</i>	62
<i>Table 5.1. : Simulation Inputs</i>	63
<i>Table 5.2. : Initial carbon loadings.</i>	72
<i>Table 5.3. : Steady-state carbon loadings.</i>	74

LIST OF FIGURES

	PAGE
Figure 2.1.: Diagram of the CIP process.	7
Figure 3.1.: Blank Simulink flow-sheet.	28
Figure 3.2.: Simulink Library Browser.	30
Figure 3.3.: Constant Block.	31
Figure 3.4.: Mux block and Demux block linked via signal line.	31
Figure 3.5.: Scope block.	31
Figure 3.6.: Add block.	32
Figure 3.7.: Subtract block.	32
Figure 3.8.: Divide block.	32
Figure 3.9.: Product block.	33
Figure 3.10.: Gain block.	33
Figure 3.11.: Integrator block.	33
Figure 3.12.: Derivative block.	34
Figure 3.13.: Compare to zero block.	34
Figure 3.14.: If then Else block.	34
Figure 3.15.: If Action Block.	35
Figure 3.16.: MinMax Block.	35
Figure 3.17.: Memory Block.	35
Figure 3.18.: Uniform Random Number and Step Change blocks.	36
Figure 3.19.: Tank.	36
Figure 3.20.: Tank model in Simulink.	37
Figure 3.21.: v1 and v2 vs. simulation time (20 000s).	38
Figure 3.22.: Tank subsystem.	40
Figure 3.23.: Tank sub-system exterior.	40
Figure 3.24.: Tank Sub-system indicating inputs on left-hand-side and outputs on right-hand-side.	41
Figure 3.25.: Stage sub-system mask.	42
Figure 3.26.: Plant parameters mask.	43
Figure 3.27.: Simulation Flow-sheet.	44
Figure 3.28.: Gold and OM sub-systems.	45
Figure 3.29.: Data inputs and outputs of a stage and its sub-systems.	47
Figure 3.30.: Sub-system hierarchy indicating the carbon loading (1), adsorption (2), leaching (3) and cyanide consumption (4) sub-systems.	48
Figure 3.31.: Gold leaching sub-system.	48
Figure 3.32.: Leaching sub-system flow sheet.	50
Figure 3.33.: Gold adsorption sub-system.	50
Figure 3.34.: Adsorption sub-system flow sheet.	52
Figure 3.35.: Carbon loading sub-system.	53
Figure 3.36.: Carbon loading sub-system.	54

Figure 3.37.: If Action sub-system.	55
Figure 3.38.: Concentration reset sub-system flow-sheet.	56
Figure 3.39.: Cyanide consumption sub-system.	57
Figure 3.40.: Cyanide consumption flow-sheet.	58
Figure 3.41.: OGR Sub-system.	59
Figure 5.1. : Carbon loading (first three stages) vs. simulation time (initial loadings equal zero).	65
Figure 5.2. : Carbon loading (last three stages) vs. simulation time (initial loadings equal zero).	66
Figure 5.3. : Saw-tooth carbon loading profile in 1 st stage.	67
Figure 5.4. : Barren solution gold concentration vs. simulation time.	68
Figure 5.5.: Saw-tooth carbon loading profile in last stage.	69
Figure 5.6.: Barren value of solids.	70
Figure 5.7.: Barren solution gold concentration.	70
Figure 5.8. : Overall gold removal percentage (initial loadings equal zero).	71
Figure 5.9. : Carbon loading (first three stages) vs. simulation time (initial loadings specified).	72
Figure 5.10. : Carbon loading (last three stages) vs. simulation time (initial loadings specified).	73
Figure 5.11. : Barren solution gold concentration vs. simulation time (initial loadings specified).	74
Figure 5.12. : Overall gold removal percentage (initial loadings specified).	75
Figure 6.1.: Step in liquid feed gold concentration.	77
Figure 6.2.: Carbon loading profiles (first three stages) resulting from step-change in liquid feed gold concentration.	78
Figure 6.3.: Barren solution concentration profile resulting from step-change in liquid feed gold concentration.	78
Figure 6.4.: Overall gold removal vs. simulation time resulting from step-change in liquid feed gold concentration.	80
Figure 6.5.: Carbon loading profiles (first three stages) corrected by stepping carbon transfer fraction.	81
Figure 6.6.: Barren solution concentration resulting from a step-change in carbon transfer fraction.	82
Figure 6.7.: Carbon loading profiles (first three stages) resulting from a step-change in transfer frequency.	83
Figure 6.8.: Barren solution concentration profile resulting from step-change in transfer frequency.	84
Figure 6.9.: Step-change in solids feed rate.	85
Figure 6.10.: Carbon loading profiles (first 3 stages) resulting from a step-change in solids feed rate.	86

Figure 6.11.: Overall gold removal vs. simulation time resulting from a step-change in solids feed rate.	87
Figure 6.12.: Barren solution concentration profile corrected by step-change in carbon transfer fraction.	88
Figure 6.13.: Carbon loading profiles (first 3 stages) corrected by step-change in carbon transfer fraction.	89
Figure 6.14.: Overall gold removal vs. simulation time resulting from step-change in carbon transfer fraction.	90
Figure 6.15.: Carbon loading profiles (first 3 stages) resulting from step-change in elution efficiency.	91
Figure 6.16.: Carbon loading profiles (last 3 stages) resulting from a step-change in elution efficiency.	92
Figure 6.17.: Barren solution concentration profile resulting from a step-change in elution efficiency..	93
Figure 6.18.: Overall gold removal vs. simulation time resulting from a step-change in elution efficiency.	94
Figure 6.19.: Carbon loading profiles (first 3 stages) resulting from a step-change in carbon transfer fraction.	95
Figure 6.20.: Controlled and un-controlled carbon loading in the first stage.	95
Figure 6.21.: Barren solution concentration profile resulting from a step-change in carbon transfer fraction.	96

NOMENCLATURE

Symbol	Description	Unit
A	Area	m ²
C _C	Carbon loading	g/t
C _L	Concentration of gold in liquid phase	g/t
C _S	Concentration of gold in solid phase	g/t
C _{p(e)}	Concentration of gold in ore at equilibrium	g/t
C _{p(t)}	Concentration of gold in ore at time t	g/t
F _C	Fraction of carbon in stage to be transferred	
h	Height	m
h ₀	Initial height	m
k _A	Adsorption rate constant	s ⁻¹
K _A	Adsorption equilibrium constant	
k _L	Leaching rate constant	s ⁻¹
K _L	Leaching equilibrium constant	
L	Liquid flow rate	t/s
M	Mass per stage (used with subscript)	t
S	Solids flow rate	t/s
t _i	Carbon transfer interval	s
v	Volumetric flow rate	m ³ /s
V	Volume	m ³
SUBSCRIPTS		
in	Value entering stage	
out	Value leaving stage	
N	Referring to stage number	
C	Carbon	
CN ⁻	Cyanide	
L	Liquid phase	
S	Solid phase	
OM	Other metals (Used only when excluding gold)	
ABBREVIATIONS		
CIC	Carbon-in-Column	
CIL	Carbon-in-Leach	
CIP	Carbon-in-Pulp	
OGR	Overall Gold Removal	

Introduction

1.1. Background

The CIP process is firmly established in gold producing countries all over the world. The carbon-in-pulp process recovers gold from solution by adsorbing gold onto activated carbon and separating the two by screening. Since its inception in the early 1960's, the CIP process has undergone a lot of transformation and fine-tuning.

The CIP process is complex, since the overall efficiency is governed by numerous inter-dependant variables and processes. The large number of factors which dictate the dynamics of the system makes the process difficult to optimize and control.

1.2. Project Motivation

CIP technology is firmly entrenched in the mining sector due to numerous advances in the last few decades. Powerful computing techniques and software has made it possible for plant simulations to accurately predict real plant dynamics. This provides crucial insight during normal operation and the design stage.

Introduction

The large number of factors that dictate plant dynamics makes the process difficult to optimize and control. It therefore becomes necessary to establish simulation techniques whereby real plant behavior can be approximated, in a dynamic environment, without the use of complex models. Many models used today are limited in their applicability (van Deventer *and* Ross, 1991). Where a fundamental modeling approach is used, models often contain factors that are difficult to measure or interpret, making them impractical for use on a large scale.

In addition, some simulation packages that are available are difficult to implement and require extensive training before it can be used correctly. These packages are also limited in versatility. The user is not exposed to the construction or inner workings of the simulation. Hence, it is not possible to conduct a “what if” simulation on all the variables present.

The CIP section of a gold plant requires thorough understanding, as this section ultimately dictates dissolved gold losses. This project is aimed at providing additional understanding of the dynamic behavior of the CIP process. It is intended that this project will result in a flexible, user-friendly simulation of the process that can be used as a design aid.

Introduction

A dynamic simulation will enable operators and engineers to run start-up simulations, investigate control strategies, simulate periodic carbon transfers and investigate the addition of cyanide to any stage at any time (Simulation time). It is also possible to conduct investigations on the influence of any variable that is time dependant or stage-number dependant.

1.3. Objectives

The objective of this study is to evaluate the effectiveness and versatility of a dynamic CIP process simulation, using Simulink in Matlab. An empirical approach is taken based on simplicity. This leads to a powerful, uncomplicated solution that can be used by plant personnel to examine and predict the effect of disturbances on the dynamics of the system.

Rate and equilibrium parameters are calculated from plant data, in Simulink, by minimizing the error between actual and predicted outputs, using Matlab's built in search algorithms. Hence, the empirical model implicitly incorporates variables like oxygen addition. The flexibility of Simulink allows the user to look into the effects of a change in any parameter on plant performance, which must ultimately be maximized.

Introduction

The applicability of the simulation will be assessed quantitatively, by subjecting the system to variations in operating conditions.

1.4. Plan of Development

The literature review of this report will provide a brief description of the CIP and CIL process, plant operation and models that were used. The literature review includes a description of the solution methods utilized by Matlab.

The Methodology section encompasses the modeling and simulation considerations, simplifying assumptions and mass-balance equations. The reader is exposed to the Simulink environment and some of the most commonly used blocks. The method of simulation construction in Simulink is explained with the help of an unsteady-state tank example. The simulation architecture is explained in terms of layout, variable inputs and outputs, sub-system blocks and their flow-sheet layouts.

Simulation results are presented and compared to actual data. The effects of some disturbances to the system are investigated. These disturbances are countered in various ways.

Finally, relevant comments and recommendations are made.

Literature Review

2.1. The Carbon-in-Pulp Process

Carbon adsorption recovery includes the following branches: carbon-in-pulp (CIP), carbon-in-leach (CIL) and carbon-in-column (CIC). The CIL process is the result of combining adsorption and leaching into one circuit.

Filtration followed by zinc precipitation has been the method of recovery for more than 80 years. Since its inception in the 60's, CIP processes have become the preferred method of gold recovery due to its simplicity, reduced capital cost, reduced operating cost and insensitivity to tonnage changes (Bailey, 1987).

The CIP method of recovery is generally used to treat low-grade ore feed. Granular activated carbon, made from wood, nut-shells, coal or coke, is passed counter-current to cyanide in adsorption contactors.

The CIP process most widely used in South Africa consists of the following major unit operations:

- 1) Pre-screening
- 2) Carbon adsorption
- 3) Carbon acid-washing and elution
- 4) Gold electrowinning or precipitation, and
- 5) Carbon reactivation

Literature Review

The gold bearing ore is crushed, then finely ground to around 75 microns size, with water added to form a slurry or 'pulp'. The pulp is dosed with cyanide, and agitated through a series of tanks. In the process it leaches the gold from the ore particles into solution. This process is termed cyanidation. On completion of cyanidation the pregnant pulp is transferred to the CIP process. The pregnant pulp is passed progressively through a number of tanks in series (generally around 5 or 6) which are situated on a sloped surface. These are mechanically stirred, or air agitated. Granulated carbon is passed through the tanks counter-current to the flow of the pulp. The granulated carbon is of a significantly larger particle size than the ground ore particles. This allows the carbon to be pumped counter current to the pulp through the use of screens sized to allow the finely ground ore to flow through and the coarser carbon to be contained. As the carbon passes through the tanks (up the train) it collects increasing quantities of gold from solution, finally reaching its highest loading value in the first tank (Bailey, 1987). The loaded carbon is separated from the pulp in the final tank and transferred to the elution circuit. The barren pulp is dewatered, to recycle water and cyanide for reuse in the process, and the remainder, termed tailings, is transferred to the tailings dam. The tailings will also contain cyanide (Mintek, 2004)

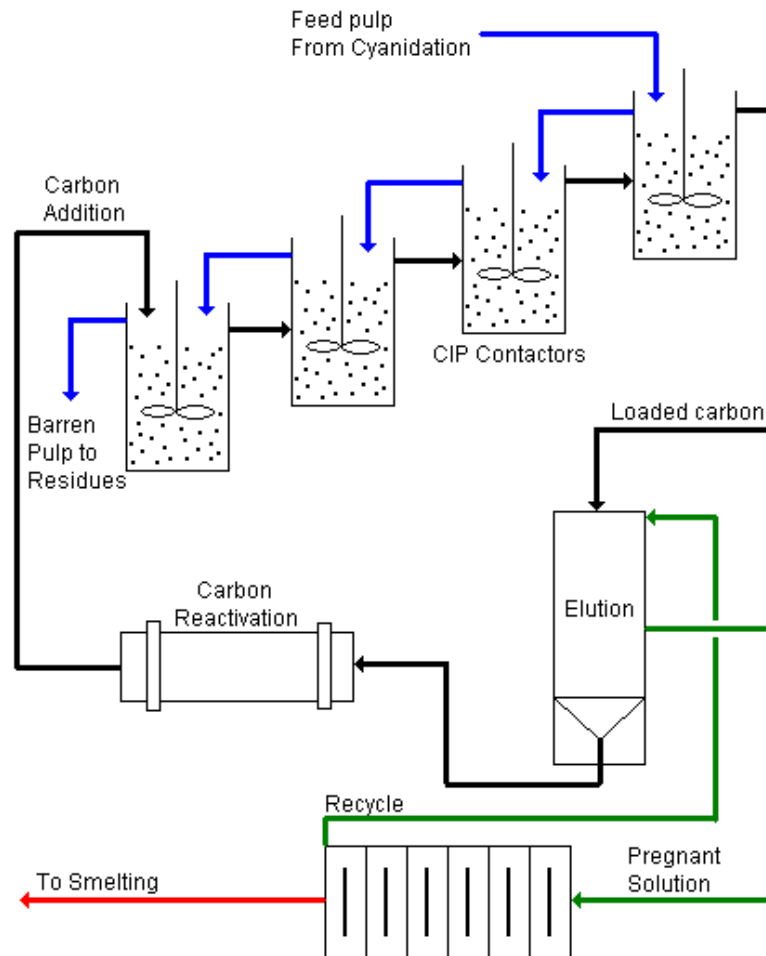
Literature Review

Figure 2.1.: Diagram of the CIP process (Mintek, 2004).

The loaded carbon is treated in the elution circuit with a hot cyanide and caustic solution to remove the gold from the carbon. The barren carbon is transferred to the reactivation circuit and then reused in the CIP process. The cyanide and caustic solution is passed through an electrowinning circuit where the gold is transferred to steel wool (or alternatively, it can be precipitated using zinc dust). The barren cyanide and caustic solution is recycled to the elution circuit.

Literature Review

The gold plated steel wool is transferred to the smelting circuit to produce gold bullion (Mintek, 2004).

This project is primarily concerned with the adsorption stage of the process. The simulation as described in this project is set up as a CIP/CIL system (where the pulp contains cyanide). Hence, leaching and adsorption takes place simultaneously in each contacting stage. The efficiency of the pulp-carbon contact in the adsorption stage governs the recovery of soluble and adsorbed gold from the pulp. Gold is lost in the tailings pulp via fine carbon that carries gold. Apart from this, the undissolved gold in the pulp also results in losses. Gold locked up in carbon as a result of inefficient elution will result in decreased adsorption kinetics.

This operation usually occurs in a number of adsorption vessels in series. Leached pulp is counter-currently contacted with activated carbon. Carbon transfer occurs intermittently, hence the process never truly reaches steady-state. Nevertheless, steady-state is used to describe the behaviour of the system under normal operating conditions. The pulp concentration decreases as it moves down the train to give the barren values in the last stage. Carbon loading increases as it moves up the train. Only a fraction of the carbon in each stage is passed up the train when transfer takes place. Carbon is retained by screens. The slurry and carbon are kept in suspension by mechanical mixers.

Literature Review

2.2. The Carbon-in-Leach Process

The addition of carbon direct to the leaching circuit has become an attractive alternative to using separate leaching and adsorption circuits. Although this process has its advantages in terms of lowered capital cost, the process becomes considerably more complex. This inevitably leads to a number of operational problems, as the number of variable parameters increase.

It has been attempted in the past to model the carbon-in-leach process by combining suitable rate expressions for gold leaching and adsorption with the relevant mass balance equations (Nicol, Fleming and Cromberg, 1984)

The successful operation and design of the CIL process is very dependent on the leaching profile (Bailey, 1987). Some ores leach very rapidly. If this changes and gold dissolution occurs down the train, insufficient stages remain to recover the gold released.

The operation of the Beatrix CIL plant indicated that the advantages of CIL are offset by a number of disadvantages:

- Process control and operation require a great deal of understanding.
- Capital costs are lower, but can be quickly offset by high operational gold losses.

Literature Review

- Carbon and gold inventories are higher and their associated problems greater.
- The low carbon concentration increases transfer times, with more back mixing, giving poorer results.
- Leaching and adsorption requirements may be in conflict and optimisation of these stages cannot easily be achieved.

2.3. CIP/CIL Modelling

A successful CIP plant's adsorption section is expected to extract more than 99.6 % of the gold present in the solution. The large amount of inter-related factors present must be well understood to achieve good plant operation and design. They include factors such as gold content of the carbon feed, gold content of the solution feed, carbon activity, solution barren value, gold content of the loaded carbon, carbon inventory, gold lock-up and the number of stages. Changes in any one of these factors will affect the others (Bailey, 1987).

In general, increasing the amount of stages results in:

- Less carbon required to achieve the same barren.
- Higher gold value on the carbon in each stage.
- Lower weighted average gold on carbon for the system as a whole.
- Less gold lock-up.
- Less carbon abrasion and gold loss.

Literature Review

- Shorter carbon retention time and thus lower poisoning potential.

Increasing the gold loading on carbon gives:

- Little change in the carbon inventory.
- Increases the gold loading in all the stages.
- Decreases the amount of carbon transferred for elution each day.
- Increases the carbon retention time.
- Increases carbon abrasion and gold loss.
- Increases carbon poisoning potential.

A lower barren gold value can be obtained by increasing the amount of carbon present in each stage. This results in:

- A lower loading in each stage.
- An overall increase in gold lock-up.
- Longer carbon retention times.
- An increase in carbon inventory.
- More abrasion and associated gold loss and poisoning potential.

(Bailey, 1987)

In addition to the above mentioned factors, the process is made considerably more difficult to model as a result of the carbon movement in the system. Carbon

Literature Review

is transferred intermittently; hence, the system is a dynamic one which never attains a true steady-state. When the carbon is transferred, a certain percentage of the carbon inventory in each tank is passed up the train to result in counter-current carbon flow. Hence, a decreased average loading of gold on carbon is created in each stage. These phenomena have to be accounted for in order to achieve a realistic industrial-scale CIP/CIL model or simulation.

2.4. Adsorption Kinetics

An adsorption model, known as the updated “*kn*” model, has been presented by Nicol, Flemming and Cromberg (Nicol *et. al.*, 1984). The model is given by :

$$\frac{dC_L}{dt} = k [K \cdot C_L - C_C] \quad (1)$$

Where :

- k is the rate constant
- K is the equilibrium constant
- C_L is the concentration of gold in solution (g.t⁻¹)
- C_C is the gold loading on carbon (g.t⁻¹)

It was shown that the equation can be used to describe the rate of gold loading onto carbon for constant gold concentration in solution. The model includes the equilibrium loading by making use of a unitless, linear equilibrium factor, K.

This model linearly relates the adsorption rate to the distance from equilibrium.

Literature Review

In CIP operations where loading of gold is not allowed to reach equilibrium, film diffusion predominates the overall adsorption rate. Physical aspects like mixing, pulp density, carbon particle size and carbon concentration overshadow chemical considerations under these conditions. Adsorption circuits that operate close to equilibrium are governed by loading capacity. Hence, factors that effect loading capacity dictate extraction rates under these conditions (Bailey, 1987).

2.5. Leaching Kinetics

Various gold leaching models have been proposed in the past by Schubert *et. al.* (1993) and Habashi (1966). Most of these models are relatively complex to solve and require a number of parameters like surface areas, diffusivities, occlusion factors and particle radii to be determined or estimated. These models are difficult to apply practically. As a result, semi-empirical rate expressions are used more often.

An empirical rate expression has been developed at Mintek and has the following form:

$$\frac{dC_p^t}{dt} = k_p [C_p(t) - C_p(e)] \quad (2)$$

Where $C_p(t)$ is the concentration in the ore at time t

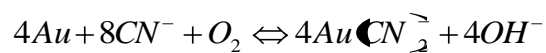
$C_p(e)$ is the concentration in the ore at equilibrium

Literature Review

k_p is a rate constant

(Bailey, 1987)

The stoichiometric relationship between gold and cyanide consumption can be given by Elsner's equation :



The amounts of solid gold, dissolved cyanide and oxygen play an important role in kinetics and equilibrium. It is assumed that oxygen is present in excess and does not have any significant impact on the rate of leaching.

From equation no. 3 it can be seen that the reaction is reversible and that equilibrium of the reaction is a function of the amounts of solid gold and gold cyanide present.

Equilibrium = $f(C_S, C_L, C_{CN^-})$, Assuming excess O_2

Assuming a linear isotherm:

$$K_L C_S = \frac{C_L}{C_{CN^-}} \quad (3)$$

Where C_S : Gold concentration on solids (g/t)

C_L : Gold concentration in liquid (g/t)

C_{CN^-} : Cyanide concentration in liquid (g/t)

Literature Review

This implies that an increase in gold or cyanide concentration will increase the distance from equilibrium and vice versa. Similarly, an increase in aurocyanide concentration will decrease the distance from equilibrium and vice versa.

If it is assumed that the rate of the reaction is a linear function of the distance from equilibrium we obtain the following rate equation:

$$\frac{dC_s}{dt} = k_L \left(K_L C_s - \frac{C_L}{C_{CN^-}} \right) \quad (4)$$

Where k_L : Leaching rate constant

K_L : Leaching equilibrium constant

2.6. Other Metals

Many other metallic species are also present, including iron, copper, nickel and silver, which must be accounted for in the cyanide balance. For simplicity it was decided to lump these various species together as a single metal M of valence +2.



A similar lumping of metallic species in CIP/CIL operations has been proposed in the past (Shubert *et al*). Leaching therefore consists of two reactions, each with its own kinetic and equilibrium parameters, that compete for available cyanide.

Literature Review2.7. Solution Methods of Matlab Simulink

The solution methods used by Simulink are imbedded in the Matlab functionality. Simulink simulates a dynamic system by computing its states at successive time steps over a specified time frame, by using the information provided by the model. The optimal solution method differs from one system to another; hence Simulink provides a set of programs, known as “solvers”, that each embody a particular solution method. These solvers incorporate numerical techniques to solve ordinary differential equations (ODE’s) that represent the continuous states of a dynamic system.

Simulink solvers fall into two main categories; fixed step and variable step. Fixed step solvers solve the model at regular time intervals. In general, decreasing the step size increases accuracy and increases solution time. Specifying a variable step solution method enables the solver to decrease the time step when the model states are changing rapidly and increase the time steps when the states are changing slowly. This method is computationally less intensive (Matlab Help,2005). The selection is made based on model behavior and the required accuracy.

Furthermore, Simulink provides both discrete and continuous solvers. In this project a continuous solution strategy was used. Continuous solvers make use of

Literature Review

numerical integration methods to determine a model's continuous states at the current time step from the states at previous time steps and the state derivatives (Matlab Help,2005).

The solver utilized in this project is ODE45 (Dormand-Prince), which is a continuous solver. It is based on an explicit Runge-Kutta (4,5) formula and it is a one-step solver. To compute y at t_n it only needs the solution at the immediately preceding time point ($y(t_{n-1})$).

ODE45 is a general application, medium scale algorithm. It provides a reasonable trade-off between accuracy and computation speed and is also the first solution method that should be tried with any system in Simulink. In this project, step size is set to variable. Beginning at the initial time with initial conditions, it steps through the time interval, computing a solution at each time step. If the solution for a time step satisfies the solver's error tolerance criteria, it is a successful step. Otherwise, it is a failed attempt; the solver shrinks the step size and tries again (Matlab Help, 2005)

The ODE45 routine is more suitable for use with non-stiff problems.

For a stiff problem, solutions can change on a time scale that is very short compared to the interval of integration, but the solution of interest changes on a

Literature Review

much longer time scale. Methods not designed for stiff problems are ineffective on intervals where the solution changes slowly because they use time steps small enough to resolve the fastest possible change (Matlab Help).

Changeable parameters include:

- Fixed or variable step
- Maximum step size
- Minimum step size
- Initial step size
- Relative tolerance
- Absolute tolerance

Simulink's Parameter Estimation toolbox is used to estimate and calibrate model parameters from experimental data. It provides the tools to:

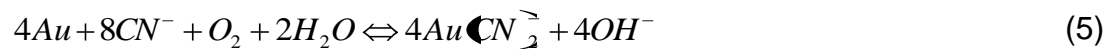
- Set up the problem
- Specify the model parameters to estimate
- Import and preprocess the experimental data
- Follow the estimation progress
- Validate the estimation results through various plots

Literature Review

Parameter estimation uses optimization routines to determine the minimum or maximum of the objective functions, by minimizing or maximizing general nonlinear functions. Functions for nonlinear equation solving and least-squares (data-fitting) problems are also provided (Matlab Help, 2005).

Methodology**3.1. Modelling Considerations**

The stoichiometric relationship between gold and cyanide consumption can be given by (Bailey, 1987):



The amounts of solid gold, dissolved cyanide and oxygen play an important role in kinetics and equilibrium. It is assumed that oxygen is present in excess and does not have any significant impact on the rate of leaching.

Various gold leaching models have been proposed in the past by Schubert *et al* (1993) and Habashi (1966). Most of these models are relatively complex to solve and require a number of parameters like surface areas, diffusivities, occlusion factors and particle radii to be determined or estimated. These models are difficult to apply practically and as a result, a semi-empirical leaching model that requires fewer parameters to obtain dissolution rates was used.

From equation 5 it can be seen that the reaction is reversible and that equilibrium of the reaction is a function of the amounts of solid gold and gold cyanide present. Therefore:

$$Equilibrium = f(C_S, C_L, C_{CN^-}), \text{ Assuming excess } O_2$$

Methodology

Where C_S is the gold concentration on solids (g/t)

C_L is the gold concentration in liquid (g/t)

C_{CN^-} is the cyanide concentration in liquid (g/t)

Assuming a linear isotherm:

$$K_L C_S - \frac{C_L}{C_{CN^-}} \quad (6)$$

This implies that an increase in gold or cyanide concentration will increase the distance from equilibrium and vice versa. Similarly, an increase in aurocyanide concentration will decrease the distance from equilibrium and vice versa.

If it is assumed that the rate of the reaction is a linear function of the distance from equilibrium we obtain the following rate equation:

$$\frac{dC_S}{dt} = k_L \left(K_L C_S - \frac{C_L}{C_{CN^-}} \right) \quad \left[\frac{g}{t.hr} \right] \quad (7)$$

Where k_L is the leaching rate constant (s^{-1})

K_L is the leaching equilibrium constant

Many other metallic species are also present, including iron, copper, nickel and silver, which must be accounted for in the cyanide balance. For simplicity it was

Methodology

decided to lump these various species together as a single metal M of valence +2 and average weight 60 g/mol.

The reaction stoichiometry is given by:



Leaching therefore consists of two reactions, each with its own kinetic and equilibrium parameters, that compete for available cyanide. These four parameters must be determined from data before leaching rates can be predicted. The cyanide concentration is implicitly linked to both reactions in the simulation.

The adsorption model selected for this study is that proposed by Nicol *et al* (1987) and was selected based on its simplicity. Once again, the rate is a linear function of the distance from equilibrium.

$$\frac{dC_L}{dt} = k_A (K_A C_L - C_C) \quad \left[\frac{g}{t.hr} \right] \quad (9)$$

Where C_C is the carbon loading (g/t)

k_A is the adsorption rate constant (s^{-1})

K_A is the adsorption equilibrium constant

Methodology

Again, four parameters must be solved in order to predict sorption rates. That is, rate and equilibrium parameters for both gold and M.

There are numerous variables that affect the CIP/CIL process, such as:

- pH
- carbon fouling
- preg-robbing
- pore structure of carbon
- carbon transfer rates / loading frequency
- competitive adsorption
- carbon breakage mechanisms
- equilibrium conditions
- carbon activity

However, some of these variables are also present when we determine our overall rate and equilibrium parameters and can be said to be implicitly incorporated into the kinetic and equilibrium parameters. These parameters are not likely to have an adverse affect on the system's response to the disturbances we are concerned with. For this reason the simulation makes use of the following simplifying assumptions:

- No adverse pH changes are present

Methodology

- Adsorption and leaching kinetics are explained by a linear rate equation (Concentration difference between source and destination phase)
- The effect of fouling on mass transfer kinetics and equilibrium is constant
- Carbon breakage can be expressed as a fixed percentage of the amount of carbon transferred with carbon fines gold loading equal to the gold loading in the final stage.
- Perfect mixing
- The effect of back mixing is negligible
- Carbon activity remains constant

3.2. Mass Balances

Mass balances are performed for both gold and the other metal species (OM) in each phase (liquid, solids and carbon). Perfect mixing is assumed and therefore exit concentrations are equal to the concentrations inside the stage. Steady-state is assumed to prevail for the duration of each time-step, provided that the time-step is sufficiently small. Accumulation terms then become negligible.

The sets of mass balance equations are identical for gold and OM, since they are both subjected to leaching and adsorption. They differ only in kinetic and equilibrium parameters and are linked through cyanide consumption, which in turn affects the leaching kinetics.

Methodology**3.2.1. Mass Balances for Gold and OM**

(Note: The text will progressively define nomenclature as they appear.)

(Concentration terms may refer to either gold or OM. Their mass balances differ only with respect to the values assigned to their kinetic and equilibrium parameters.)

In the solid phase:

$$0 = S.C_{S,N-1} - S.C_{S,N} - k_L \left(K_L.C_{S,N} - \frac{C_{L,N}}{C_{CN^-,N}} \right) . M_S \quad (\text{g/s}) \quad (10)$$

Where S : Solids flow rate (t/s)

L : Liquid flow rate (t/s)

M : Mass per stage (Solids or Liquids indicated by subscript) (t)

k_L : Leaching rate constant (s^{-1})

K_L : Leaching equilibrium constant

k_A : Adsorption rate constant (s^{-1})

K_A : Adsorption equilibrium Constant

C: Concentration (Referring to either gold or OM) (g/t)

Subscripts S: Solid phase

L: Liquid phase

C: Carbon phase

N: Stage number

CN⁻: Cyanide

In the liquid phase:

$$0 = L.C_{L,N-1} - L.C_{L,N} + k_L \left(K_L.C_{S,N} - \frac{C_{L,N}}{C_{CN^-,N}} \right) M_S - k_A (C_{L,N} - C_{C,N}) M_L$$

(g/s)

(11)

In carbon:

The process, as set up in the simulation, is unsteady with respect to carbon loading. Carbon transfer occurs every t_i seconds where fraction F_C of the carbon from stage $N+1$ is transferred to stage N (counter-current). The initial carbon loading for stage N is re-calculated every t_i seconds in the following manner:

$$C_{C,N,t=0} = C_{C,N,t=t_i} \cdot (1 - F_C) + C_{C,N+1,t=t_i} \cdot F_C \quad (\text{g/t})$$

(12)

Where F : Fraction of Carbon per stage that is transferred every t_i seconds

t_i : Transfer time (s)

At this point it is necessary to clarify the concept of simulation time in Matlab Simulink. Simulink conducts a 500 000 s dynamic simulation in a very short time, depending on the complexity of the simulation. Simulation time has no bearing on real-world time.

Methodology

With a transfer time of 2700 s and a simulation time of 500 000 s, carbon transfer will occur 185 times during the course of the simulation.

Carbon loading in stage N at simulation time is given by:

$$C_{C,N,t=t} = \frac{C_{C,N,t=0} \cdot M_C + \int_{t=0}^{t=t} k_A \left(C_{L,N} - C_{C,N,t=t} \right) \dot{M}_L}{M_C} \quad (\text{g/t}) \quad (13)$$

Where t is the transfer time. This effectively gives a saw-tooth carbon loading profile over time in every stage.

3.2.2. Cyanide Consumption

From equations 5 and 8 it can be seen that cyanide reacts with gold in molar ratio 2:1 and in ratio 3:1 with M^{2+} . A cyanide mass balance over stage N yields:

$$0 = L C_{CN^-,N-1} - L C_{CN^-,N} - 1.3 k_{L,OM} \left(C_{S,OM,N} - C_{L,OM,N} \right) \dot{M}_S - 0.2653 k_L \left(C_{S,N} - C_{L,N} \right) \dot{M}_S$$

(g/s) (14)

Subscript OM refers to Other Metals.

3.2.3. Overall Gold Removal

The overall gold removal is calculated in the following manner:

Methodology

$$OGR(\%) = \left[\frac{(L.C_{L,Feed} + S.C_{S,Feed}) - (L.C_{L,N=6} + S.C_{S,N=6})}{(L.C_{L,Feed} + S.C_{S,Feed})} \right] \cdot 100 \quad (15)$$

The gold removal is based purely on leaching and adsorption efficiency.

3.3. Simulink Interface

The Simulink interface allows a user to graphically program functions. Functions are constructed by dragging various basic blocks onto the flow-sheet and linking them to manipulate input signals to obtain the desired output. Functions can be grouped together in subsystems. A subsystem is the graphical equivalent of a “procedure” in Turbo Pascal or a “Sub” in Visual Basic. Just like procedures, subsystems can contain more subsystems.

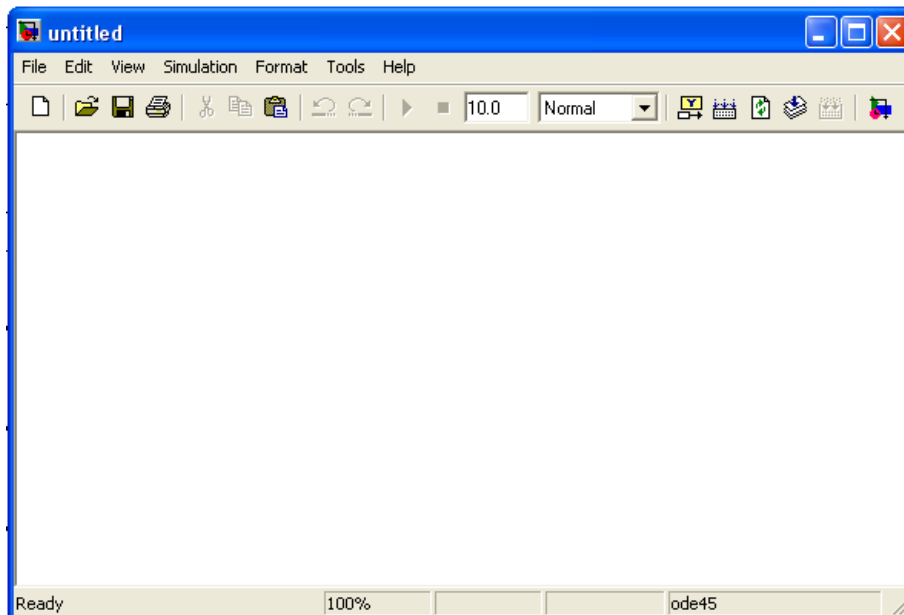


Figure 3.1.: Blank Simulink flow-sheet.

Methodology

It is important to bear in mind that Simulink is merely a GUI programming tool which is built on top of Matlab. Simulink uses either medium or large-scale search algorithms, built into Matlab, to solve unknowns (exit concentrations).

Another important concept in Simulink is simulation time. This allows the user to conduct dynamic simulations. The user is able to investigate the behavior of the system, or fluctuations of a certain variable, over the specified simulation time (time dependant variables). Matlab is able to simulate long simulation times in a matter of seconds. Simulation time has no bearing on real-world time.

The blocks necessary for constructing models in Simulink are found in the Simulink Library Browser (Figure 3.2.). The left-hand-side contains the library directories. It essentially groups related blocks. The blocks themselves can be found on the right-hand-side. Real time simulations can acquire inputs through a server (OPC toolbox). Offline simulations acquire their inputs through data files or by specifying input parameters in the Matlab workspace or within a “constant” block in Simulink.

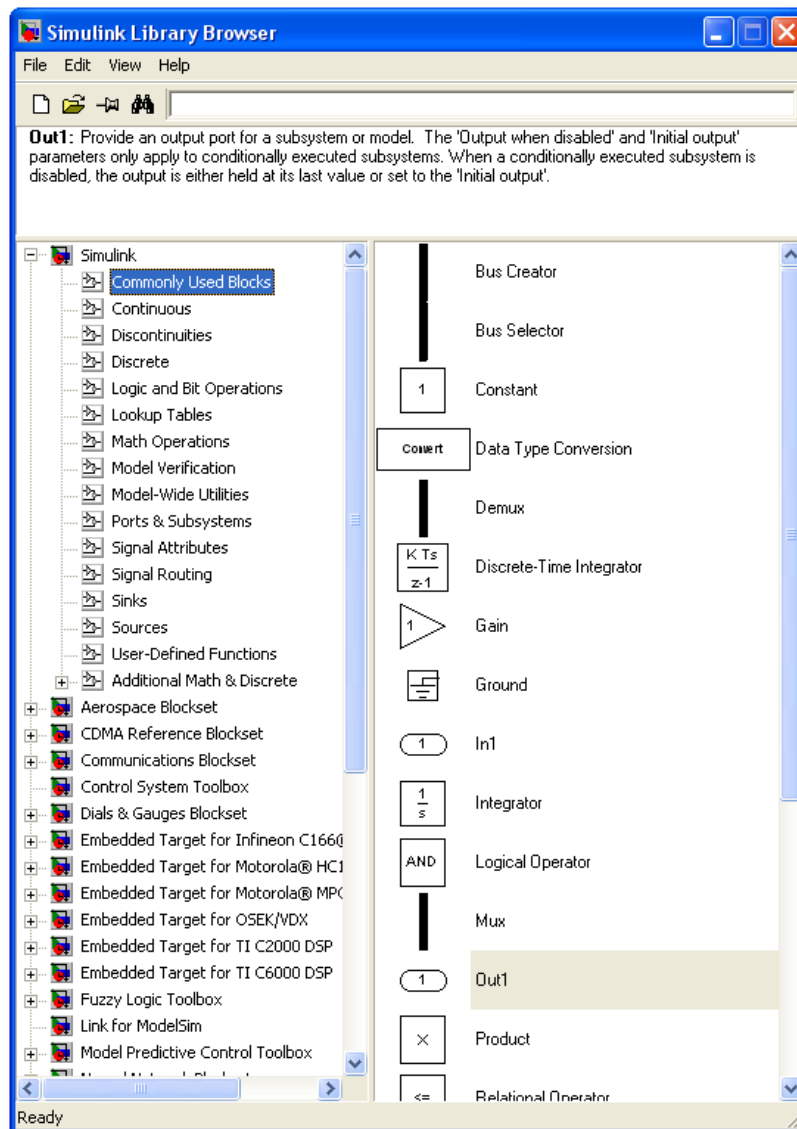
Methodology

Figure 3.2.: Simulink Library Browser.

Methodology

Here follows a list of the most commonly used blocks in the CIP/CIL process simulation:



Figure 3.3.: Constant Block (Sources directory).

Contains either a value or a variable name which has been defined in the Matlab workspace. Used as an input block.

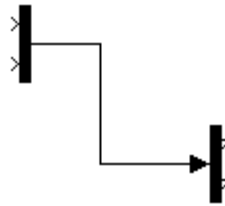


Figure 3.4.: Mux block (LHS) and Demux block (RHS) linked via signal line.

The Mux block groups various (2 or more) inputs into a single signal line and the Demux block de-groups the inputs in the same order. Used mostly to prevent simulation flow-sheets from looking cluttered and to send two or more signals into a block or subsystem through a single in-port.



Figure 3.5.: Scope block (Sinks directory).

Methodology

A Scope block can be attached to a signal to plot the signals' value over time. It can also be attached to the output of a Mux block to plot various signals on one graph. Simulation time is plotted on the X-axis.



Figure 3.6.: Add block (Math operations directory).

Adds two (or more) signals connected to it on the left-hand side to produce the sum on the right-hand side.



Figure 3.7.: Subtract block (Math operations directory).

Gives the result of top input minus bottom input (LHS). Result on right-hand side.



Figure 3.8.: Divide block (Math operations directory).

Divides the top input by the bottom input.



Figure 3.9.: Product block (Math operations directory).

Multiplies two or more inputs.



Figure 3.10.: Gain block (Math operations directory).

Acts as an in-line multiplier. It can contain either a numeric value or a variable which has been defined in the workspace.



Figure 3.11.: Integrator block (Continuous directory).

Accumulates its input signal over time. Initial conditions can be specified internally or externally. Enabling external initial condition source gives the block an extra in-port on the left-hand side. Can also be set to “resetable”. This resets the integrator block to its initial value when some external event occurs.



Figure 3.12.: Derivative block (Continuous directory).

Outputs the rate of change of the input signal w.r.t. time.

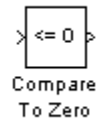


Figure 3.13.: Compare to zero block (Logic and bit operations directory).

Gives a Boolean output (true or false) based on the specified condition. If the condition is ≤ 0 , then an input of -1 will give an output of “true”.

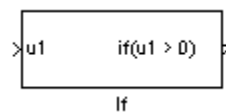


Figure 3.14.: If then Else block (Ports and Subsystems directory).

Used in combination with “If Action” subsystem (below). If a specified condition is true, then the “If Action” block manipulates a signal in a certain manner.

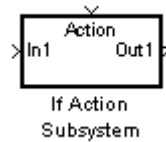


Figure 3.15.: If Action Block (Ports and Subsystems directory).

Top in-port receives a Boolean signal. If the block becomes activated, the left-hand side in-signal is manipulated according to function constructed inside the block. It can have multiple inputs and outputs. The block behaves like a subsystem, but it only manipulates a signal (or lets a signal through) when some external event triggers it.



Figure 3.16.: MinMax Block (Math operation directory).

Keeps track of either the minimum or the maximum of all the values that have passed through it.



Figure 3.17.: Memory Block (Discrete directory).

Outputs the input from the previous time step when used with discrete model simulations. Also useful for specifying the initial condition of a signal.

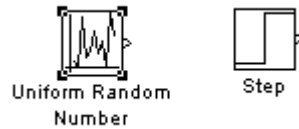


Figure 3.18.: Uniform Random Number and Step Change blocks (Sources directory).

Allows the user to investigate the effects of disturbances on the dynamics of the process simulation.

At this stage it is necessary to discuss an example to make some of the concepts more clear.

3.3.1. Tank Example

We have a tank with a height of 2 m and a base area of 1 m^2 .

We want to monitor the level in the tank.

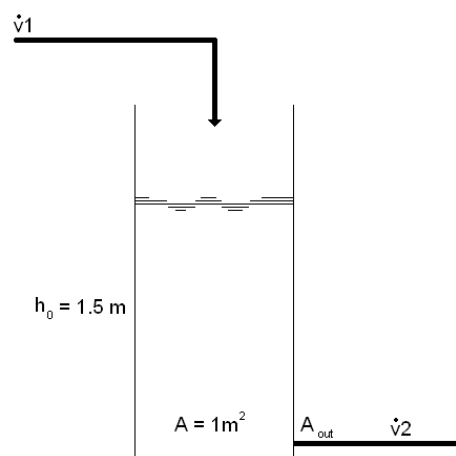


Figure 3.19.: Tank.

Methodology

$$\text{Let } \dot{v}_2 = A_{out} \sqrt{2gh} \quad (16)$$

A balance over the tank yields:

$$\frac{dV}{dt} = \dot{v}_1 - \dot{v}_2 \quad (17)$$

$$\therefore A \frac{dh}{dt} = \dot{v}_1 - A_{out} \sqrt{2gh} \quad (18)$$

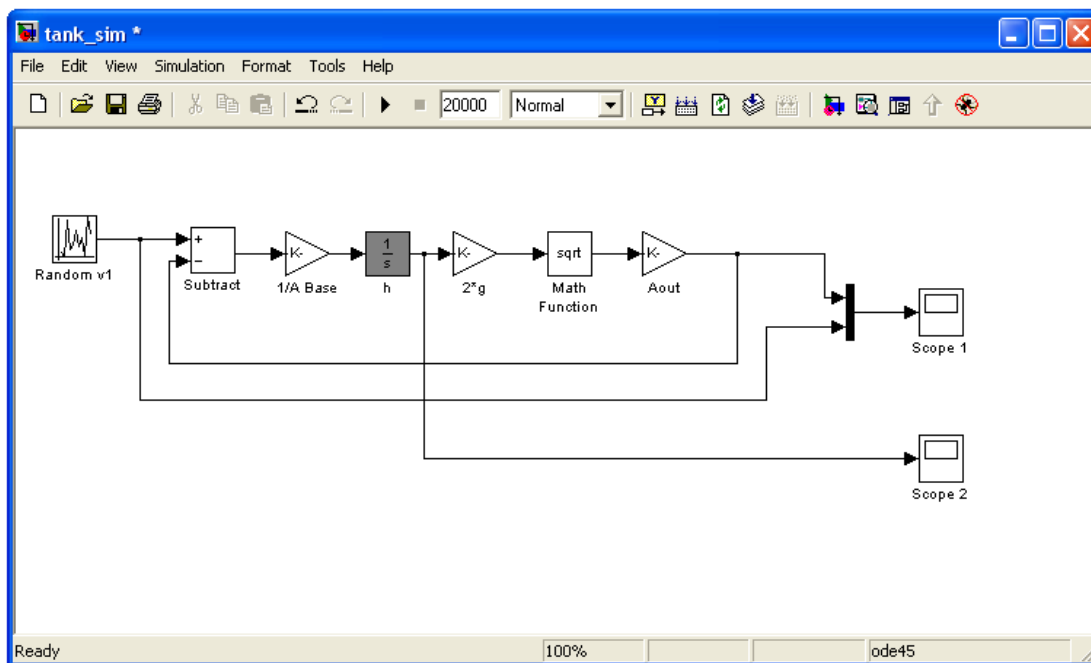


Figure 3.20.: Tank model in Simulink.

The integrator block (grey) is given an initial height. The height is used to determine the flow out of the tank. This value is then subtracted from the flow into the tank to obtain change in volume. The change in volume is divided by the cross sectional area of the tank to obtain the change in height. This can have either a positive or a negative value. The value is sent to the integrator block,

Methodology

which determines the new height inside the tank. Scope block 1 plots v_1 and v_2 vs. simulation time and scope block 2 plots h vs. simulation time.

The following inputs were given:

$$h_0 : 1 \text{ m}$$

$$A_{\text{base}} : 1 \text{ m}^2$$

$$A_{\text{out}} : 0.0005 \text{ m}^2$$

V_1 is varied randomly between 0.0015 and 0.002 m^3/s every 4000 s. A simulation time of 20 000 s was used.

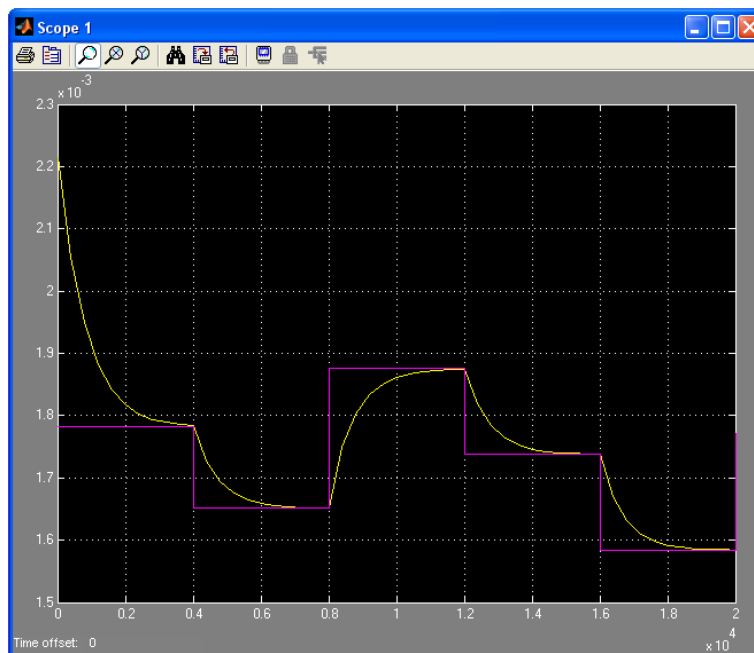


Figure 3.21.: v_1 and v_2 vs. simulation time (20 000s).

Figure 3.21. illustrates how the system strives towards steady state after each step change in inlet flow-rate.

A plot of liquid level vs. simulation time yields:

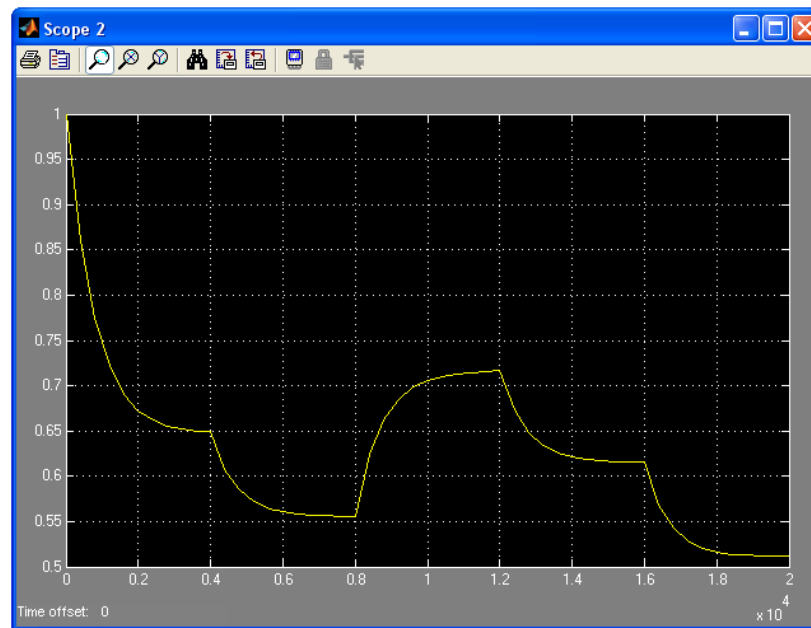


Figure 3.22.: h vs. simulation time (20 000 s).

Our model flow-sheet can be converted to a subsystem. We can then connect our tanks in series without having our flow-sheet look cluttered and confusing. In general, sub-systems are created when a specific function may be required elsewhere and needs to be duplicated.

The inside of the sub-system is illustrated in Figure 3.23.

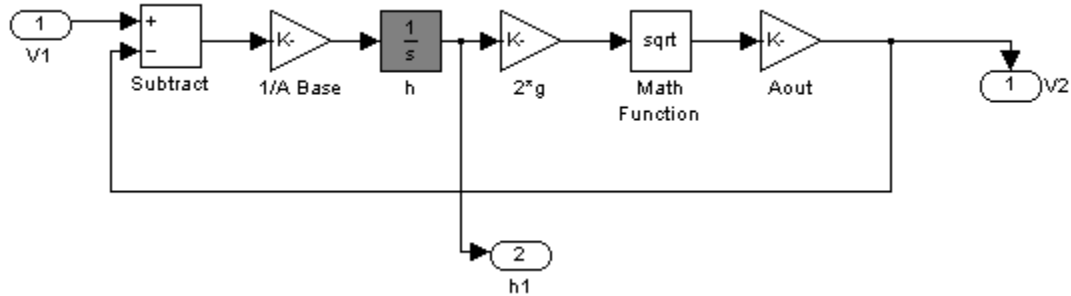
Methodology

Figure 3.23.: Tank subsystem.

Inputs and outputs are automatically detected and connected to in- and out-ports.

Externally, the sub-system looks as follows:

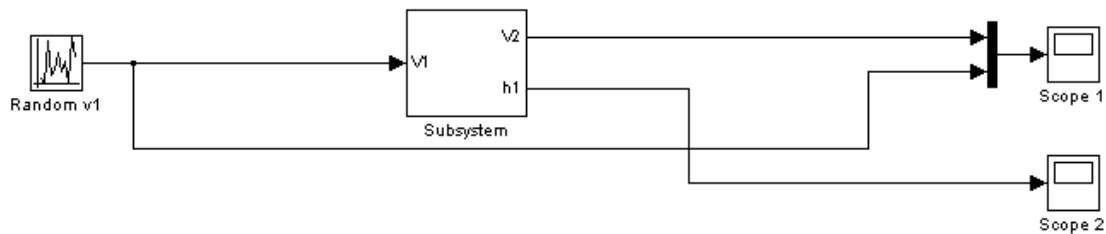


Figure 3.24.: Sub-system exterior.

3.4. Simulation Architecture3.4.1. Stage Block

Six stages were used in the simulation. Every stage is a masked sub-system, hence inputs that are relevant to that stage can be entered in the mask. This eases the process of manually adding stages.

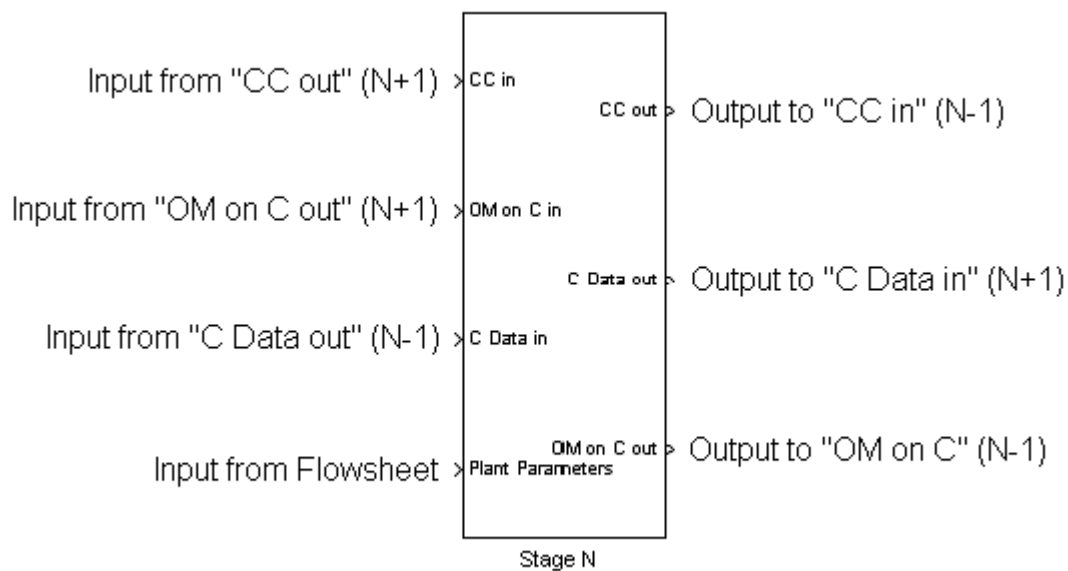


Figure 3.25.: Tank Sub-system indicating inputs on left-hand-side and outputs on right-hand-side.

Stage mask parameters are:

- Mass of solids
- Mass of liquids
- Mass of carbon in stage
- Initial carbon loading

Methodology

- Fraction of carbon that is transferred
- Cyanide concentration increase

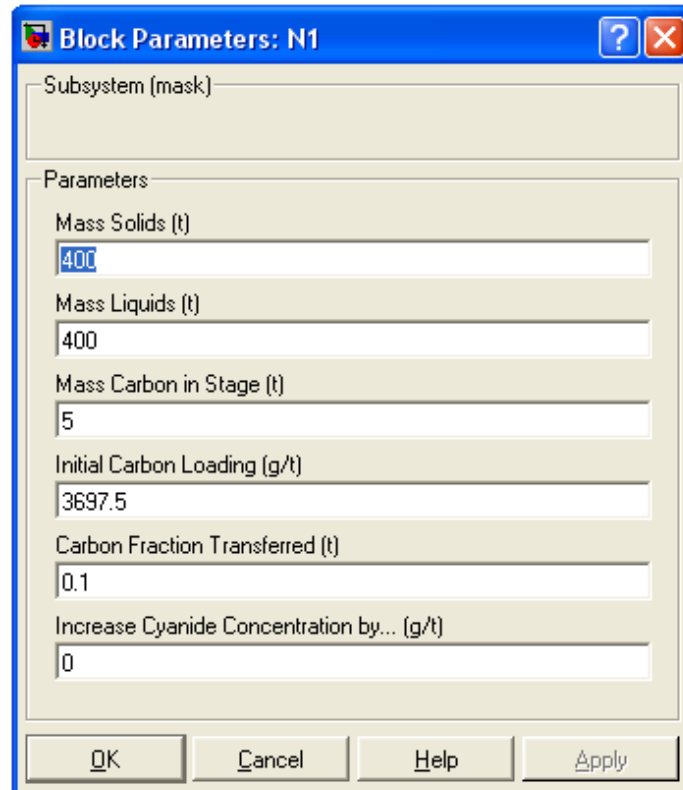


Figure 3.26.: Sub-system mask.

Furthermore, every stage also receives inputs from the preceding stage (Gold and OM concentration data), following stage (Gold and OM loading passed counter-current) and parameters that are specified in the Matlab workspace.

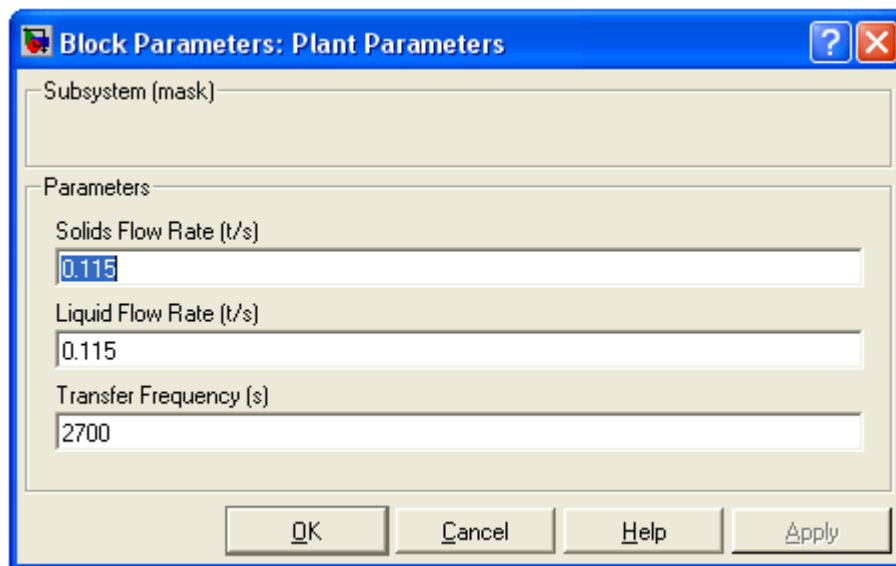
They include:

- Other metals elution efficiency
- Gold elution efficiency

Methodology

- Gold adsorption rate constant
- Gold adsorption equilibrium constant
- Gold leaching rate constant
- Gold leaching equilibrium constant
- Other metals adsorption rate constant
- Other metals adsorption equilibrium constant
- Other metals leaching rate constant
- Other metals leaching equilibrium constant

Solids flow-rate, liquid flow-rate and transfer time are entered into a separate mask in the flow-sheet.



Block Parameters: Plant Parameters

Subsystem (mask)

Parameters

Solids Flow Rate (t/s)
0.115

Liquid Flow Rate (t/s)
0.115

Transfer Frequency (s)
2700

OK Cancel Help Apply

Figure 3.27.: Plant parameters mask.

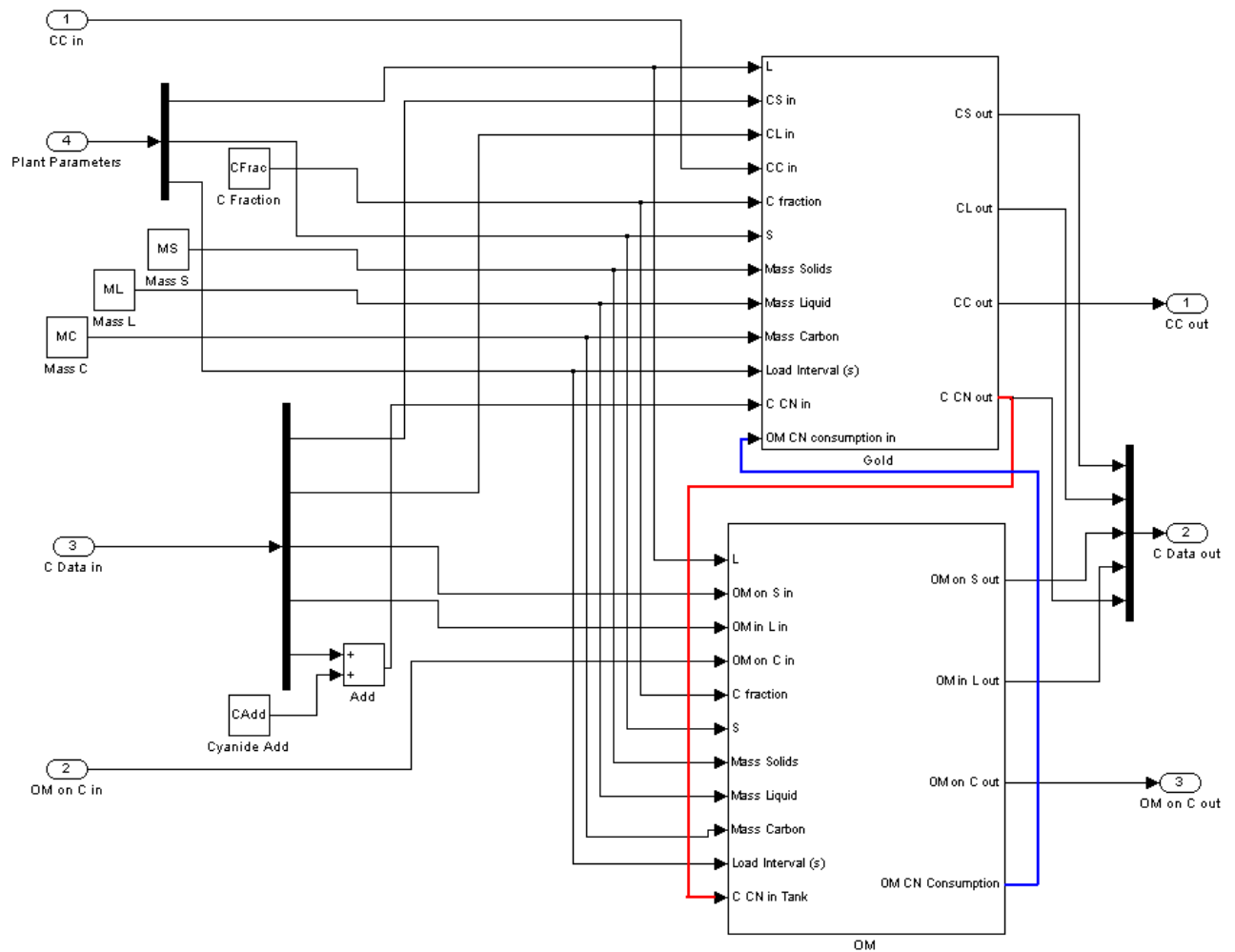
Methodology**3.4.2. Gold And OM Sub-systems**

Figure 3.29.: Gold sub-system.

Underneath the Stage sub-system lays the Gold and OM sub-systems. Their inner workings will be discussed in more detail later. For now it is sufficient to point out that these sub-systems are linked only by cyanide concentration (red) and consumption (blue). The sub-system that evaluates the combined Gold and OM consumption is located in the Gold sub-system, therefore the exit cyanide

Methodology

concentration (C CN out) is determined by the Gold sub-system. Apart from that, and kinetic and equilibrium parameters (specified in workspace), the Gold and OM sub-systems receive identical inputs with respect to operating parameters (specified in sub-system mask).

They are (refer to Figure 3.29.):

- Liquid flow-rate (L)
- Solids flow-rate (S)
- Carbon transfer fraction (C Fraction)
- Mass of solids in stage (Mass Solids)
- Mass of liquid in stage (Mass Liquids)
- Mass of carbon in stage (Mass Carbon)
- Load interval
- Cyanide concentration (C CN in) (Only in Gold sub-system)

Concentration data (Gold and OM in liquid and solids) that is passed to a stage (from stage N-1 or Feed input) is de-mixed and distributed to their relevant input ports (LHS : C Data in). Output concentration data is mixed together and passed to the next stage (RHS : C Data out). Refer to Figure 3.25.

The mixed concentration data consists of:

- Other metals on Solids (OM on S,OM sub-system)

Methodology

- Other metals in Liquid (OM in L,OM sub-system)
- Gold on solids (CS in, Gold sub-system)
- Gold in liquid (CL in, Gold sub-system)
- Cyanide in liquid (C CN in, Gold sub-system)

Gold and OM loading on carbon (CC and OM on C) are passed individually and from stage N+1 to stage N.

The constant blocks on the left-hand-side of Figure 3.29. contain stage parameters which are entered via the stage mask.

Both the Gold and OM sub-systems each conceal a leaching sub-system, adsorption sub-system and carbon loading sub-system. These Sub-subsystems have identical flow-sheet layouts for Gold and OM. As mentioned, their inputs differ only with respect to kinetic and equilibrium parameters and concentrations, as Gold and OM concentrations are treated separately. For this reason, only the Gold sub-system will be discussed. It should be pointed out that only the Gold sub-system contains a cyanide consumption sub-system.

Methodology

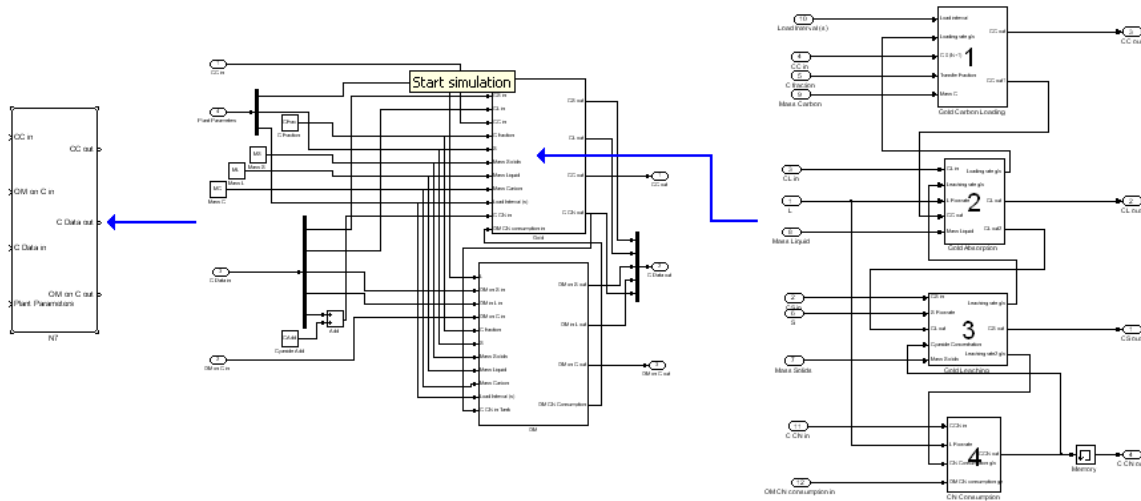


Figure 3.30.: Sub-system hierarchy indicating (on RHS) the carbon loading (1), adsorption (2), leaching (3) and cyanide consumption (4) sub-systems.

3.4.3. Leaching Sub-system

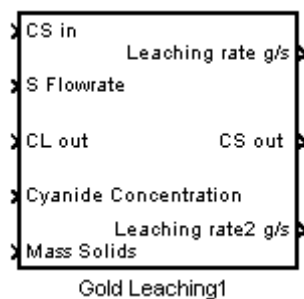


Figure 3.31.: Gold leaching sub-system.

The leaching sub-system acquires the following inputs:

- CS in (g/t) : Concentration of gold on solids in feed to stage
- CL out (g/t) : Concentration of gold in liquid in stage (hence exit concentration)

Methodology

- Cyanide concentration (g/t) : Concentration of cyanide in stage. Received from cyanide consumption sub-system.
- Mass solids (t) : Total mass of solids present in stage (as apposed to specifying stage volume and feed density)
- S Flowrate (t/s) : From plant parameters mask.

It yields the following outputs:

- Leaching rate (g/s) : Passed to the adsorption sub-system and results in an increase in dissolved gold concentration.
- Leaching rate2 (g/s) : Passed to the cyanide consumption block.
- CS out (g/t) : Exit concentration of gold on solids

“CS out” is an unknown that has to be solved for.

As mentioned before, gold and OM mass balances are performed for liquid, solids and carbon separately. The leaching sub-system evaluates mass balances over solids via the following equation:

$$0 = S.C_{S,N-1} - S.C_{S,N} - k_L \left(K_L.C_{S,N} - \frac{C_{L,N}}{C_{CN^-,N}} \right) . M_S \quad (19)$$

The flow-sheet layout of this equation is shown in Figure 3.32.

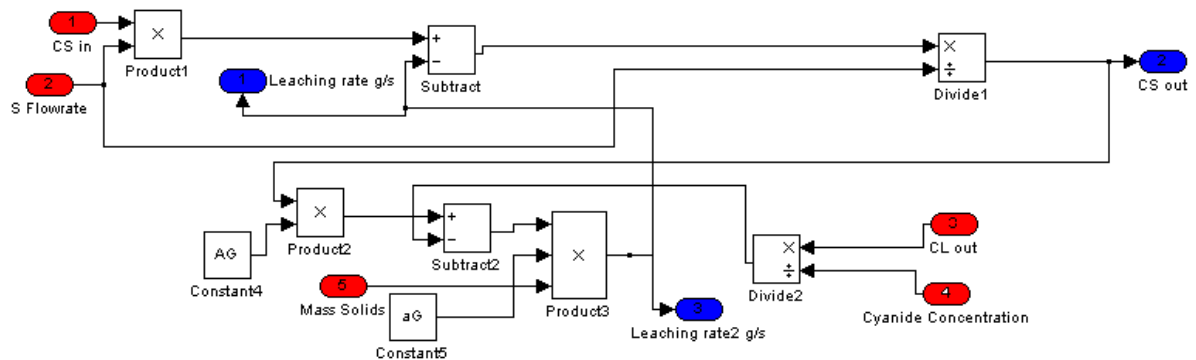
Methodology

Figure 3.32.: Leaching sub-system flow sheet (inputs : red, outputs : blue).

The sub-system determines, from CS in and S flowrate, the amount of gold (in g/s) entering the stage and subtracts the rate of leaching (in g/s) to determine the current concentration of gold on solids (CS). CS out is fed backwards and to an output port. aG and AG are rate and equilibrium constants for gold leaching. They are specified in the Matlab workspace.

3.4.4. Adsorption Sub-system

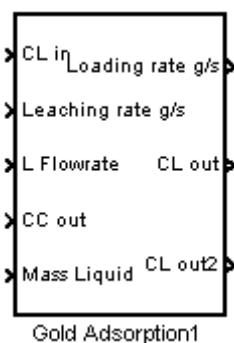


Figure 3.33.: Gold adsorption sub-system.

Methodology

The adsorption sub-system receives the following inputs:

- CL in (g/t) : Concentration of gold in liquid
- Leaching rate (g/s)
- L Flowrate (t/s) : Liquid flow rate
- CC out (g/t) : Carbon loading in stage at any time
- Mass liquid (t) : Mass of liquid present in stage

The following outputs are determined:

- Loading rate (g/s) : Rate at which gold is adsorbed onto carbon
- CL out (g/t) : Exit concentration of gold in liquid (to output port)
- CL out2 (g/t) : Becomes input to leaching sub-system

“CL out” and “CL out2” are identical. “CL out” is an unknown that has to be solved.

The adsorption sub-system constitutes mass balancing over the liquid component, as described by the following equation:

$$0 = L.C_{L,N-1} - L.C_{L,N} + k_L \left(K_L \cdot C_{S,N} - \frac{C_{L,N}}{C_{CN^-,N}} \right) M_S - k_A (C_{L,N} - C_{C,N}) M_L \quad (20)$$

The third term in the equation is obtained from the leaching sub-system.

Its flow sheet representation is illustrated by Figure 3.34.

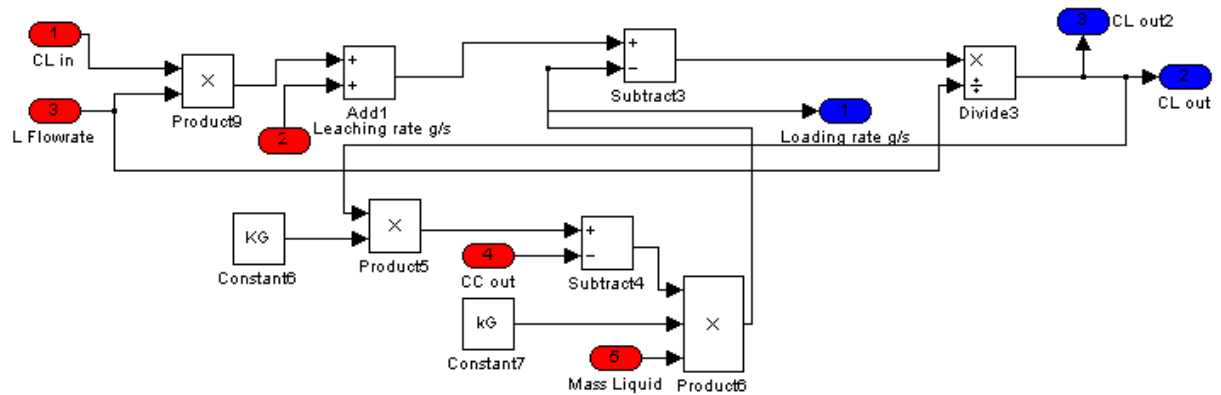
Methodology

Figure 3.34.: Adsorption sub-system flow sheet (inputs : red, outputs : blue)

The amount of gold which enters the stage through the liquid component (in g/s) is determined. Gold entering the liquid phase through leaching (in g/s) is added and the rate of adsorption (in g/s) is subtracted. This yields the amount of gold leaving the stage (in g/s). This is converted to the exit concentration of gold in the liquid phase (CL out, in g/t), which is equal to the concentration inside the stage, since it is assumed that every stage is perfectly mixed. The loading rate (in g/s) is sent to the carbon loading sub-system via an output port.

kG and KG are rate and equilibrium constants relating to loading kinetics of gold only. They are specified in the Matlab workspace.

3.4.5. Carbon Loading Sub-system

This sub-system is slightly more complex, mainly because it contains more sub-systems. It contains integrator blocks, which enables the simulation to

Methodology

accumulate gold onto the carbon in every stage. Integrator blocks are at the center of almost every dynamic simulation in Simulink.

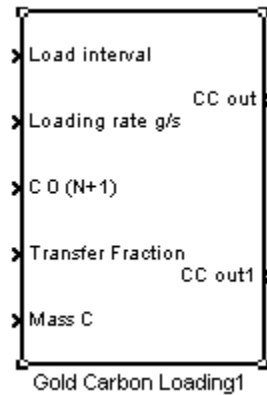


Figure 3.35.: Carbon loading sub-system.

The carbon loading sub-system receives the following inputs:

- Load interval (s) : Loading occurs from $t=0$ to $t=t_f$. Initial loading is adjusted when carbon transfer takes place.
- Loading rate (g/s) : From loading sub-system. The loading rate is accumulated to determine the overall loading of carbon in the stage.
- $C_0(N+1)$ (g/t) : Gives the maximum overall carbon loading of Stage (N+1) just before transfer occurs.
- Transfer fraction : Fraction of carbon in stage N that is transferred to stage N-1
- Mass C (t) : Mass of carbon in stage

Outputs:

- CC out (g/t) : Carbon loading

Methodology

- CC out1 (g/t) : Carbon loading. This output becomes an input to the adsorption sub-system, since adsorption kinetics depend on carbon loading.

The carbon loading sub-system, and its sub-subsystems, embodies the following equations:

$$C_{C,N,t=t} = \frac{C_{C,N,t=0} \cdot M_C + \int_{t=0}^{t=t} k_A (C_{L,N} - C_{C,N,t=t}) M_L}{M_C} \quad (21)$$

$$C_{C,N,t=0} = C_{C,N,t=ti} \cdot (1 - F_C) + C_{C,N+1,t=ti} \cdot F_C \quad (22)$$

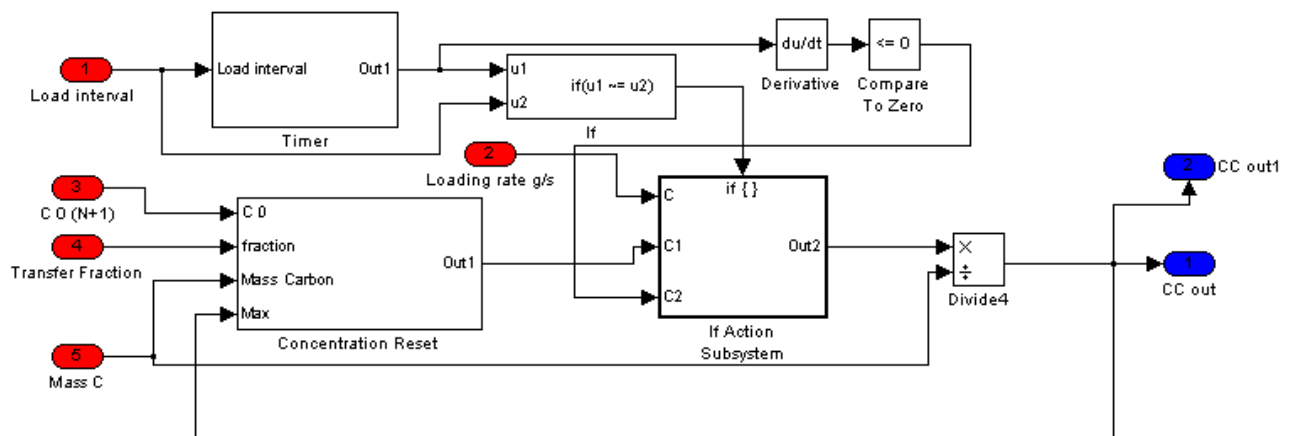


Figure 3.36.: Carbon loading sub-system (inputs : red, outputs : blue).

The carbon loading sub-system contains three more sub-systems :

- Timer
- Concentration reset

Methodology

- If Action block (regarded as a sub-system)

The Timer sub-system receives the transfer time interval and produces a saw-tooth pulse output. The output ranges between 0 and the transfer time interval (say 3000 s) and resets when the transfer time is reached. The If Action sub-system is then activated and the timer begins anew.

The If Action sub-system consists of one integrator block. It receives loading rate (in g/s), initial gold on carbon in the stage (in g, determined by the Concentration reset sub-system) and a reset signal (Boolean). The integrator block accumulates the gold on carbon in the stage. Its output is the physical amount of gold (in g) on the carbon in the stage at a specific time. It evaluates the integral in equation 21.

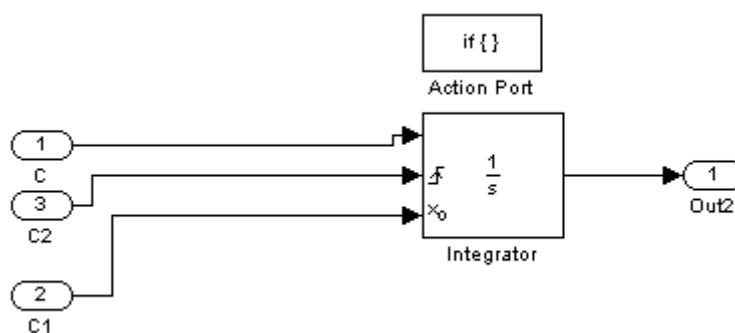


Figure 3.37.: If Action sub-system flow sheet.

Methodology

The output is converted to carbon loading (in g/t) by dividing by the amount (in t) of carbon present in the stage. This is done within the carbon loading sub-system's flow sheet.

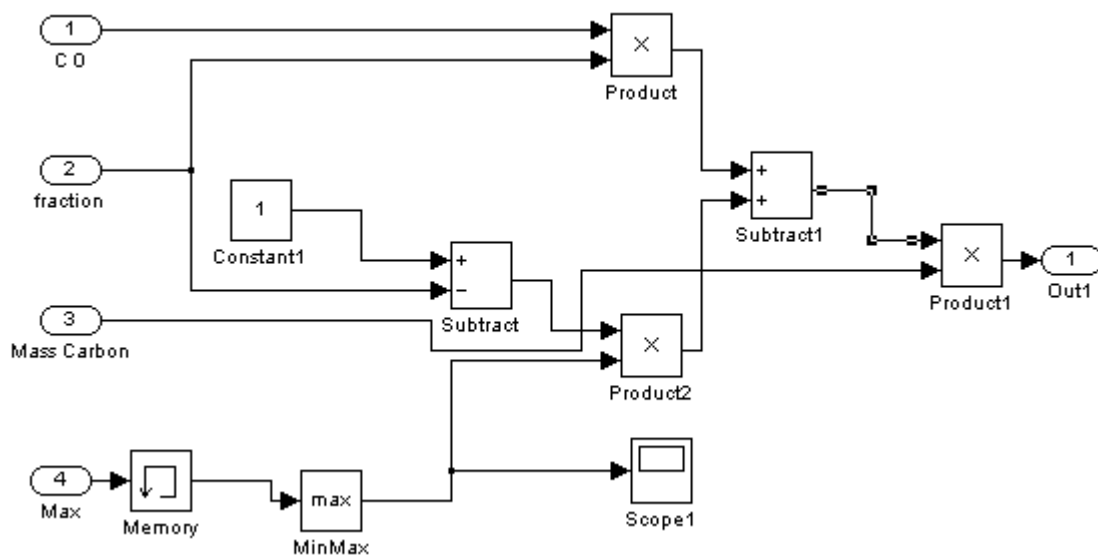


Figure 3.38.: Concentration reset sub-system flow-sheet.

The concentration reset sub-system represents equation 22. The MinMax block in the above figure records the maximum loading that is achieved between transfers in that particular stage. This value is used, together with the current loading of stage N+1 and transfer fraction, to calculate a new average loading after every transfer. It is then converted to the total gold on carbon (in g) by multiplying by the mass of carbon present in the stage. The output is continuous, but is only utilized once the “If Action” sub-system is activated.

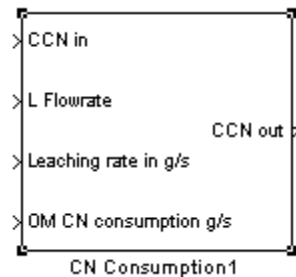
3.4.6. Cyanide Consumption Sub-system

Figure 3.39.: Cyanide consumption sub-system.

The cyanide consumption sub-system receives the following inputs:

- C CN in (g/t) : Concentration of cyanide entering the stage
- L Flowrate (t/s) : Liquid flow rate to the stage
- Leaching rate in (g/s) : Received from the leaching sub-system
- OM CN consumption (g/s) : Received from the Other Metals sub-system

Output:

- C CN out (g/t) : Concentration of cyanide inside stage (exit concentration)
- “C CN out” has to be solved.

The cyanide consumption flow-sheet is constructed to represent the following model:

$$0 = LC_{CN^-,N-1} - LC_{CN^-,N} - 1.3k_{L,OM} (C_{L,OM} C_{S,OM,N} - C_{L,OM,N}) \bar{M}_S - 0.2653k_L (C_{L,S,N} - C_{L,N}) \bar{M}_S \quad (23)$$

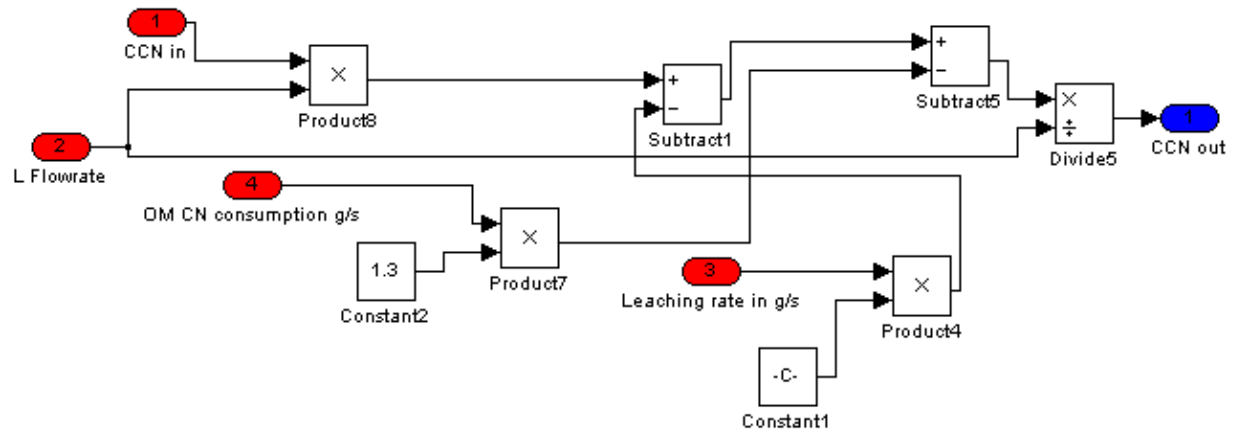
Methodology

Figure 3.40.: Cyanide consumption flow-sheet (inputs : red, outputs : blue).

The OM CN consumption input represents the third term of [equation](#). It is received from the Other Metals sub-system. The leaching rate input is acquired from the leaching sub-system and represents the fourth term in [equation](#).

The flow-sheet determines the amount of cyanide consumed, in g/s, from stoichiometry, by multiplying the gold and OM leaching rates by molar conversion factors (Molar conversion for OM = 1.3, molar conversion for gold = 0.2653).

The combined CN consumption rate is subtracted from the rate at which cyanide enters the stage. The result is divided by the liquid flow rate to obtain the exit CN concentration.

Methodology

3.4.7. Overall Gold Removal Sub-system

The Overall gold removal sub-system is situated in the main simulation flow-sheet. It embodies the following equation:

$$OGR(\%) = \left[\frac{(L.C_{L,Feed} + S.C_{S,Feed}) - (L.C_{L,N=6} + S.C_{S,N=6})}{(L.C_{L,Feed} + S.C_{S,Feed})} \right] \cdot 100 \quad (24)$$

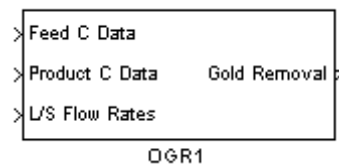


Figure 3.41.: OGR Sub-system.

It acquires concentrations of gold in the liquid and solid phase for both feed and the final product. Overall gold removal is expressed as the percentage of gold removed from the solid and liquid phase.

Results for Parameter Estimation

4.1. Modelling

Table 4.1. shows actual plant data used in determining adsorption and leaching kinetic and equilibrium parameters. Table 4.2. gives solids/liquid retention and flow specifications. Table 4.3 show intermittent carbon transfer data. Intermittent flow conditions are equivalent to a steady flow of 0.6 t/hr. Table 4.4. shows stage-by-stage adsorption data (Liquid concentration and exit carbon loading).

Table 4.1. : Actual Plant Data used for CIP Modelling.

Variable	Value	Units
Solids Feed Rate	300	t/hr
Feed Relative Density	1.45	
Solids Relative Density	2.7	
Carbon Flow Rate	0.6	t/hr
Volume per Stage	367	m ³
Head Grade	6.5	g/t
Solid Gold Loading (Feed)	1.2	g/t
Solid Gold in Effluent	0.01	g/t
Cyanide in Effluent	35	g/t
Elution Efficiency (Gold)	0.95	
Elution Efficiency (OM)	0.99	

Table 4.2. : Plant Data Converted for Simulation Input.

Variable	Value	Units
Solids Mass Fraction in Pulp Feed	0.493	
Solids Feed Rate	0.083	t/s
Liquid Feed Rate	0.086	t/s
Carbon Flow Rate	1.67E-4	t/s
Mass Solids and Liquid per Stage	532.150	t
Mass Solids per Stage	262.297	t
Mass Liquid per Stage	269.853	t

Results for Parameter Estimation

Table 4.3. : Equivalent Discrete Carbon Flow Rate.

Variable	Value	Units
Mass Carbon per Stage	5	t
Carbon Fraction Transferred	0.1	
Transfer Interval	3000	s
Discrete Carbon Flow Rate	1.67E-04	t/s

Table 4.4. : Stage-by-stage Adsorption Data.

Stage Number	$C_{L,out}$ (g/t)	$C_{C,out}$ (g/t)
Feed	5.3	175
1	1.12	3500
2	0.347	1300
3	0.064	500
4	0.017	400
5	0.01	300
6	0.003	200

A parameter Estimation was run using the above plant data and operating conditions by minimizing the error between actual and predicted values (Carbon loading in each stage, liquid gold concentration in each stage, cyanide concentration and solids gold loading in last stage).

The gold adsorption and leaching kinetic parameters were determined:

$$k_A = 7.032 \times 10^{-8} \text{ s}^{-1}$$

$$K_A = 18075$$

$$k_L = 5.847 \times 10^{-7} \text{ s}^{-1}$$

$$K_L = 2751.4$$

Results for Parameter Estimation

To ease the parameter estimation, kinetic parameters for Other Metals were not determined. It is assumed that gold is the overall rate limiting component and that the affects attributed by the Other Metal species can be neglected.

Estimates for Other Metal leaching and adsorption kinetics were taken:

$$k_{A,OM} = 5.5 \times 10^{-7} \text{ s}^{-1}$$

$$K_{A,OM} = 17000$$

$$k_{L,OM} = 1.6 \times 10^{-6} \text{ s}^{-1}$$

$$K_{L,OM} = 800$$

Table 4.5. shows a comparison between actual plant values and model outputs.

The overall gold removed from the solid and liquid streams amount to 99.84 %.

Table 4.5. : Comparison of Plant data vs. Simulated data.

Stage Number	C_L (g/t)		C_C (g/t)		C_S (g/t)		C_{CN} (g/t)	
	Actual	Sim	Actual	Sim	Actual	Sim	Actual	Sim
Feed	5.3		175					
1	1.12	1.405	3500	3300				
2	0.347	0.356	1300	640				
3	0.064	0.093	500	354				
4	0.017	0.028	400	213				
5	0.01	0.013	300	181				
6	0.003	0.01	200	172	0.01	2.4E-5	35	73.5

Results for Dynamic CIP Plant Simulation

A start-up simulation, with all initial carbon loadings made zero, was conducted with sufficient simulation time to reach steady-state. A second simulation was conducted where initial carbon loading in the stages were specified in their respective sub-system masks. Table 5.1. shows the simulation input values used.

Table 5.1. : Simulation Inputs

Parameter	Value	Units
Simulation Time	500000	s
Solids Feed Rate	0.083	t/s
Liquid Feed Rate	0.086	t/s
Mass of Solids per Stage	262	t
Mass of Liquid per Stage	269	t
Mass of Carbon per Stage	5	t
Carbon Transfer Fraction	0.1	
Intermittent Carbon Transfer Interval	3000	s
Gold Elution Efficiency	0.95	
OM Elution Efficiency	0.99	
Feed Concentration Data		
Gold on solids	1.2	g/t
Gold in Liquid	5.3	g/t
OM on solids	500	g/t
OM in liquid	100	g/t
Cyanide	800	g/t
Initial Carbon Loading ($t_{sim} = 0$)		
Stage 1	3500	g/t
Stage 2	1300	g/t
Stage 3	500	g/t
Stage 4	400	g/t
Stage 5	300	g/t
Stage 6	200	g/t
Gold Kinetic Parameters		
Leaching Rate Constant (k_L)	7.03e-8	s ⁻¹
Leaching Equilibrium Constant (K_L)	18075	
Adsorption Rate Constant (k_A)	5.84e-7	s ⁻¹
Adsorption Equilibrium Constant (K_A)	2751	

Results for Dynamic CIP Plant Simulation

Other Metals Kinetic Parameters		
Leaching Rate Constant (k_L)	1.6e-6	s^{-1}
Leaching Equilibrium Constant (K_L)	800	
Adsorption Rate Constant (k_A)	5.5e-7	s^{-1}
Adsorption Equilibrium Constant (K_A)	17000	

Note: These parameters are used throughout, except where stated otherwise.

Results for Dynamic CIP Plant Simulation

5.1. Start-up Simulation (Un-steady)

The simulation was run with all initial loadings made zero. Figures 5.1. and 5.2. show how the carbon loading in each stage strive towards a steady value. The effect of intermittent carbon transfer can be seen in the saw-tooth profile. The figures are presented separately (first 3 and last 3) for clarity.

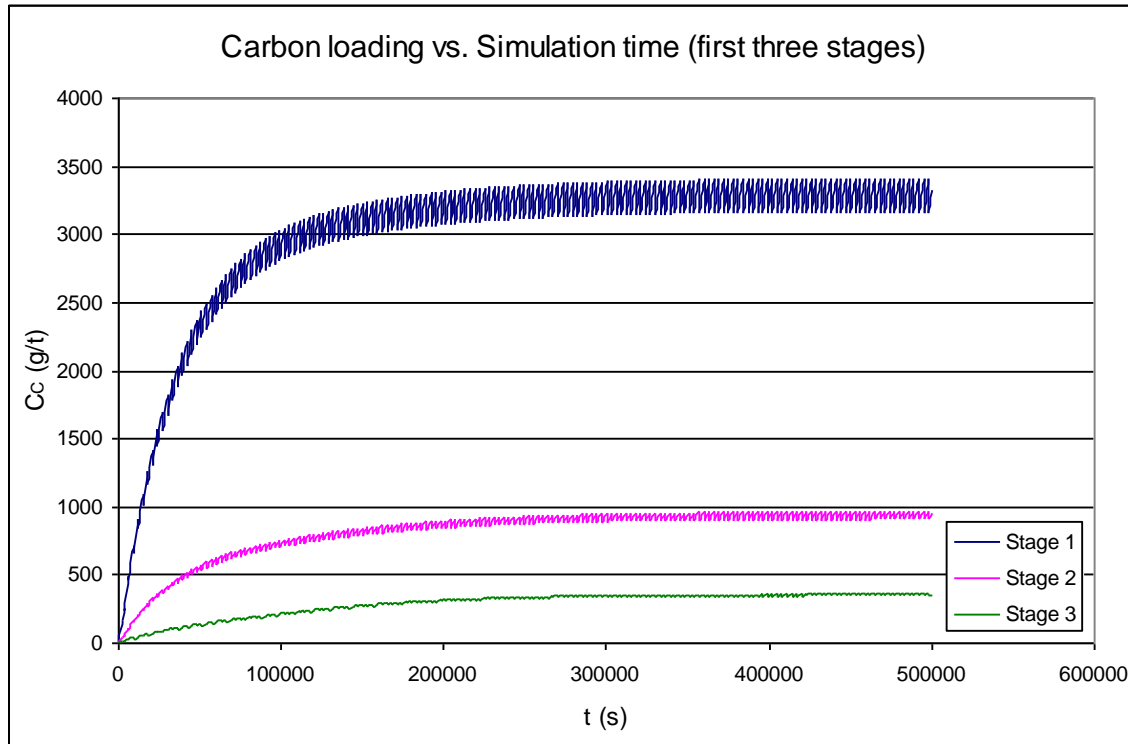


*Figure 5.1. : Carbon loading (first three stages) vs. simulation time
(initial loadings equal zero)*

Figures 5.1. and 5.2. indicate how the gold loading on carbon progressively increase in each stage until a final settling value is reached. As literature predicted, the highest loading is achieved in the first stage.

Results for Dynamic CIP Plant Simulation

Intermittent carbon transfer yields a saw-tooth loading profile against time. Once the loading profile in each stage varies between two extremes that remain more or less constant over time, the system is said to be at steady-state. View Figure 5.3. Although the system is unsteady with respect to carbon transfer, it becomes steady with respect to its inherent equilibrium conditions.

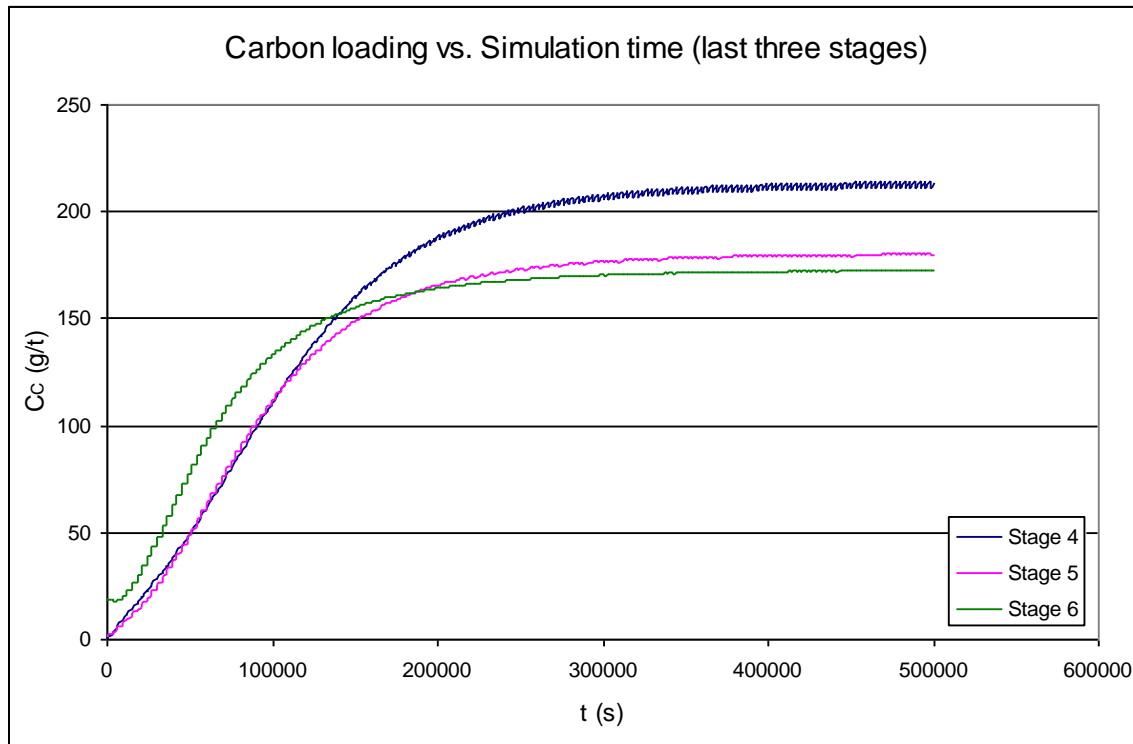


Figure 5.2. : Carbon loading (last three stages) vs. simulation time (initial loadings equal zero).

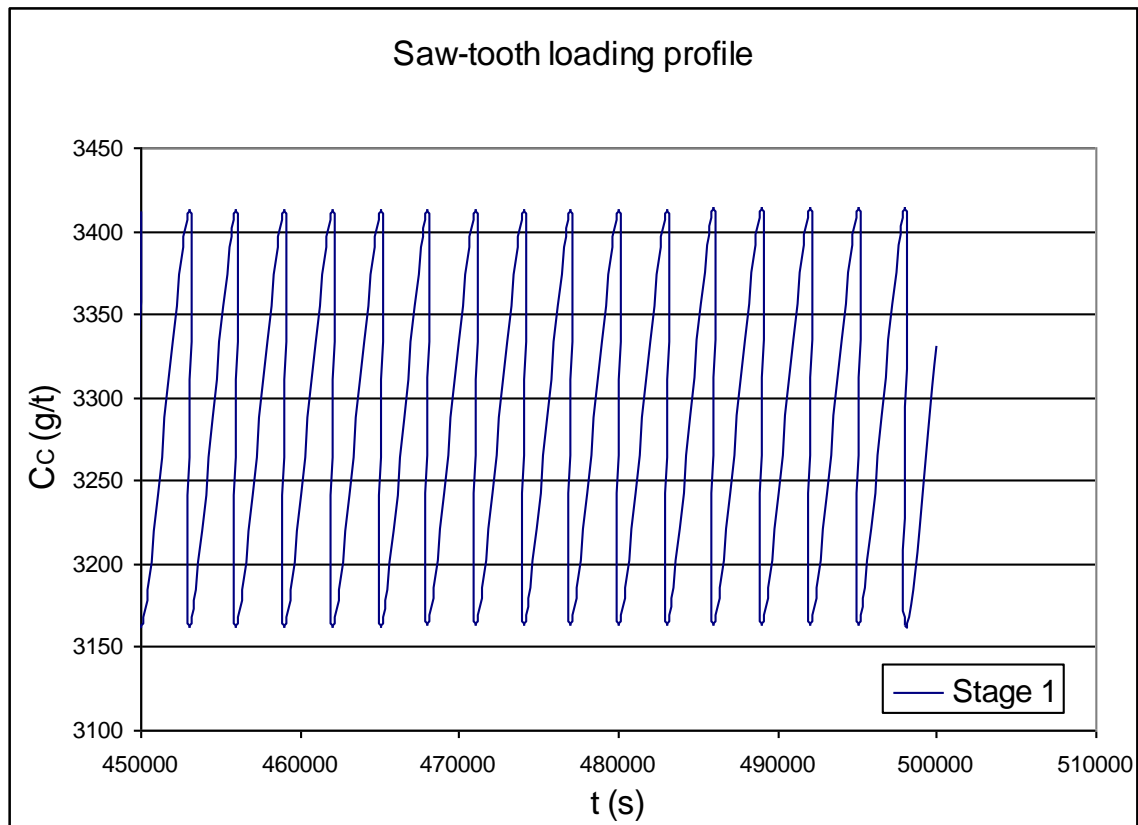
Results for Dynamic CIP Plant Simulation

Figure 5.3. : Saw-tooth carbon loading profile in 1st stage.

The carbon loading profile against time is viewed in Figure 5.3. over the last 50000 s of the time-line. The loading remains within a certain band. A valley signifies a 10% carbon transfer from stage N+1, whereas the maximum loading (peak) is reached the moment before transfer.

Results for Dynamic CIP Plant Simulation

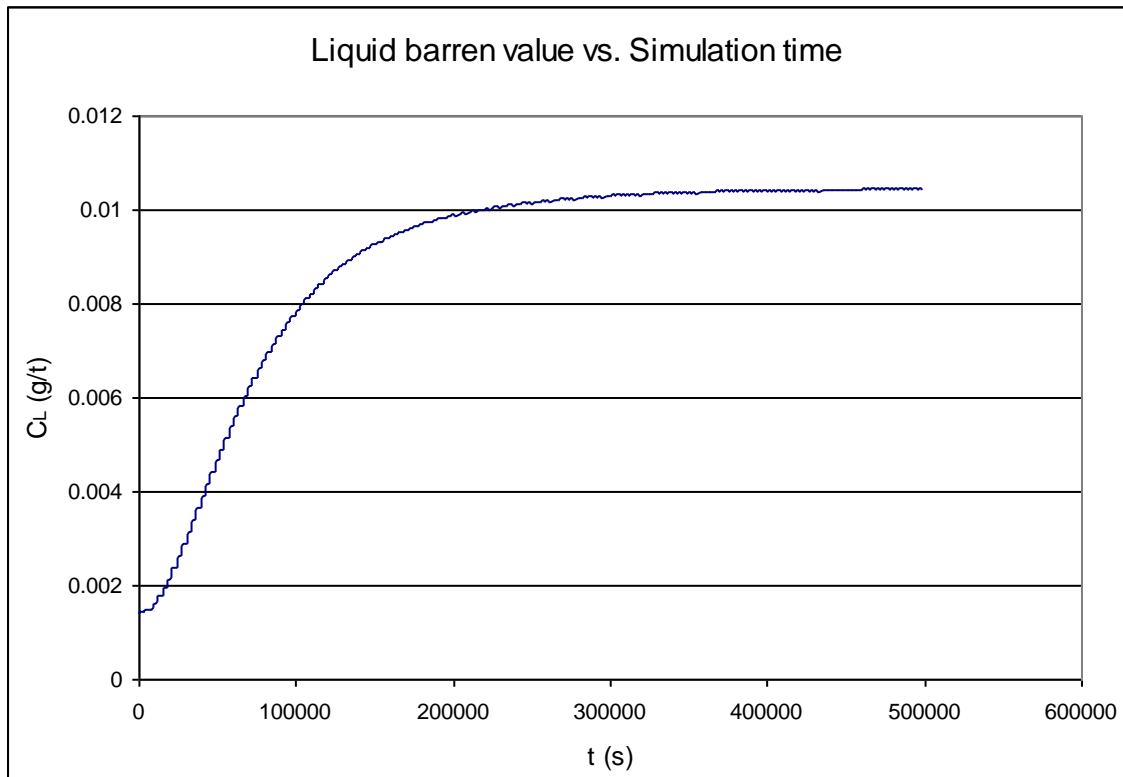


Figure 5.4. : Barren solution gold concentration vs. simulation time.

The initial barren solution concentration is low and progressively increases (Figure 5.4.). The rate of adsorption from the liquid phase decreases as the loading on carbon increases. Hence, the steady-state barren solution concentration will be higher than the initial, since the initial carbon loading in each stage is made zero.

Figures 5.5., 5.6. and 5.7. take a closer looks at the saw tooth profiles of the output concentrations (liquid, solid and carbon phase) in the last stage.

Results for Dynamic CIP Plant Simulation

The profiles are viewed over the last 20000s of simulation time. The figures indicate how the effects of intermittent carbon transfer is imposed on the leaching rate (solid phase) and adsorption rate (liquid phase). The rates of leaching and adsorption adapt to the corresponding carbon loading. When the average carbon loading is low (moment after transfer) the exit gold concentrations in the solid and liquid phase is also low. The concentrations increase as the carbon loading increases. The rate of leaching depends on the dissolved gold in the liquid phase. The rate of adsorption, again, depends on the carbon loading. Hence, the effect of carbon loading is propagated from one phase to the next.

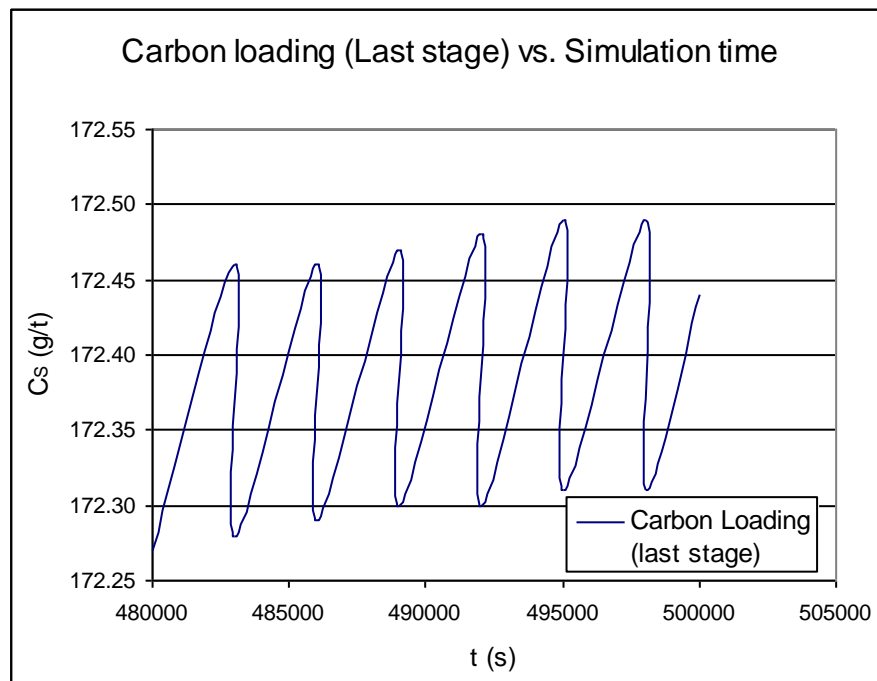
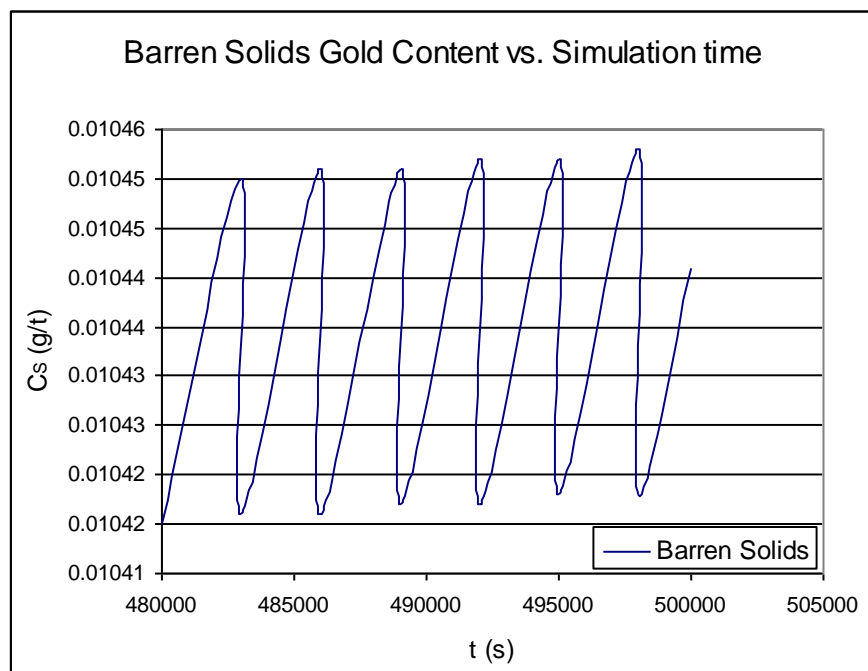
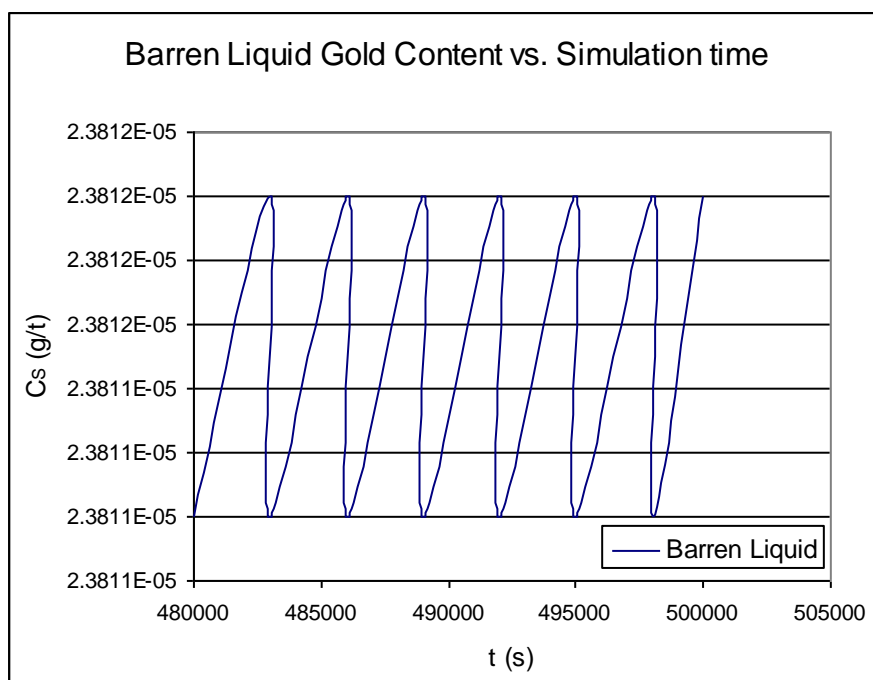


Figure 5.5.: Saw-tooth carbon loading profile in last stage.

Results for Dynamic CIP Plant Simulation*Figure 5.6.: Barren value of solids.**Figure 5.7.: Barren solution gold concentration.*

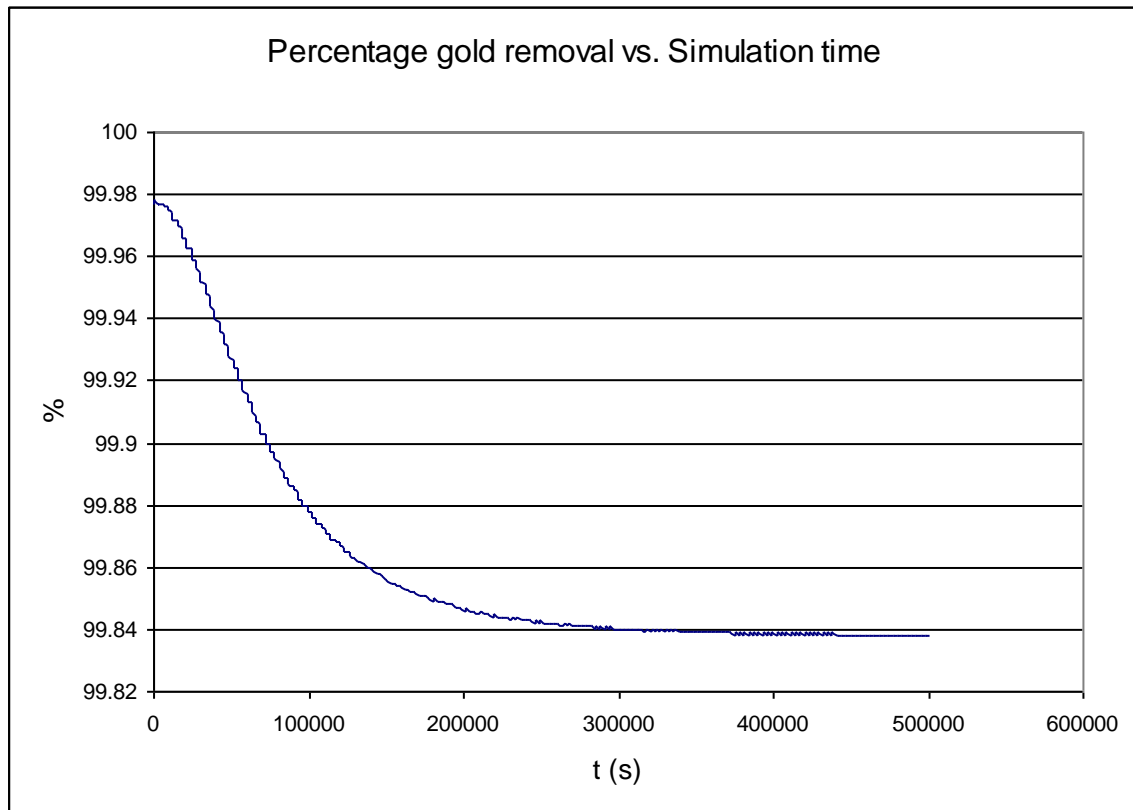
Results for Dynamic CIP Plant Simulation

Figure 5.8. : Overall gold removal percentage (initial loadings equal zero).

As expected, the initial overall gold removal is high (low barren values) and progressively decreases (barren values increase) as a result of an increase in carbon loading in each stage. Once again, a steady value is reached near the end of the simulation.

Results for Dynamic CIP Plant Simulation

5.2. Simulation Using Initial Carbon Loadings (Plant data)

The plant carbon loading data is used as initial loading values.

Table 5.2.: Initial carbon loadings.

Initial Carbon Loading ($t_{\text{sim}} = 0$)	Value	Units
Stage 1	3500	g/t
Stage 2	1300	g/t
Stage 3	500	g/t
Stage 4	400	g/t
Stage 5	300	g/t
Stage 6	200	g/t

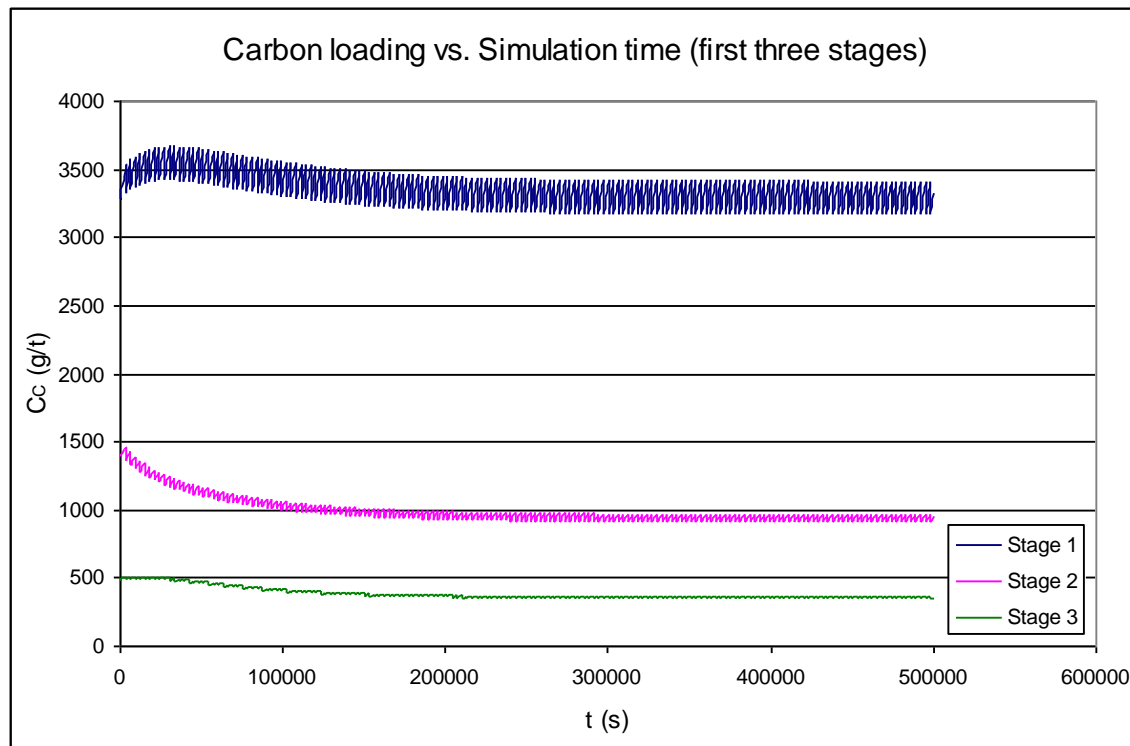


Figure 5.9. : Carbon loading (first three stages) vs. simulation time (initial loadings specified).

Figures 5.9. and 5.10. indicate how the system once again strives towards its own steady-state loading values under the same operating conditions (Table 5.1.: Simulation inputs). The bump in the carbon loading vs. time of stage one is

Results for Dynamic CIP Plant Simulation

the result of the decrease in loading of the succeeding stages, as the carbon moves up the train.

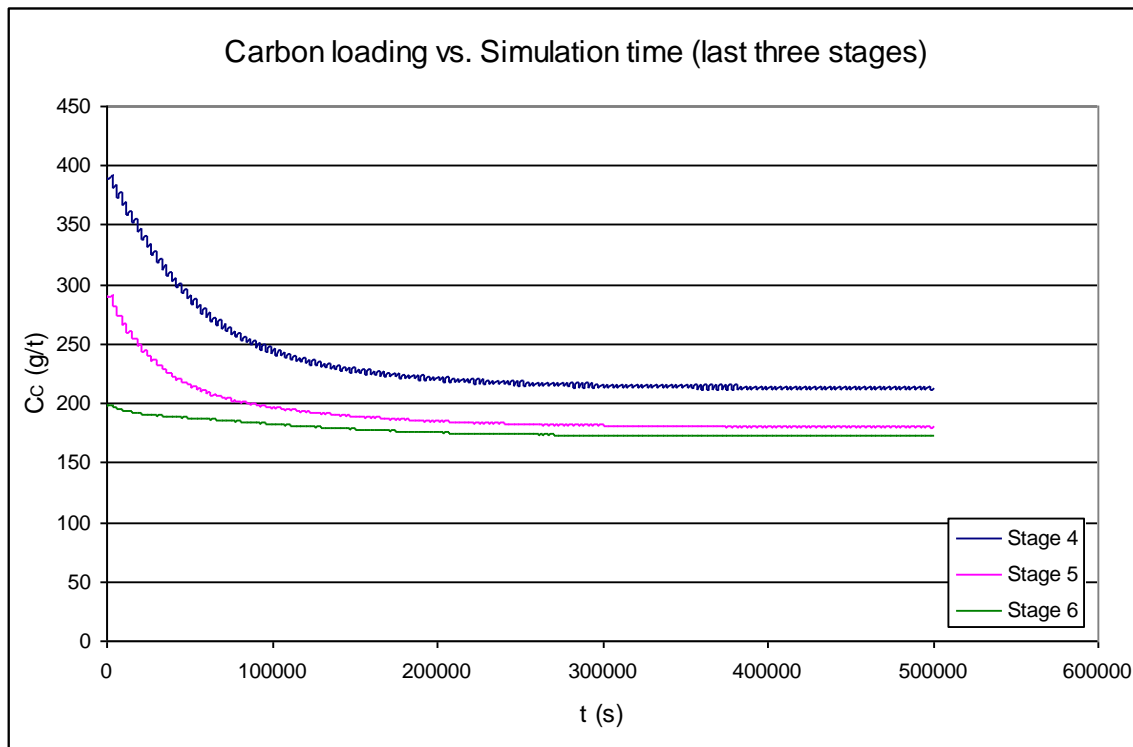


Figure 5.10. : Carbon loading (last three stages) vs. simulation time (initial loadings specified).

Regardless of the initial carbon loadings specified, the system strives towards a set of unique carbon loadings in all six stages. The results are summarized in Table 5.3. This would indicate that the simulation produces repeatable results and that these results are dependant on the specified operating conditions.

Results for Dynamic CIP Plant Simulation

Table 5.3.: Steady-state carbon loadings.

N	$C_{C,0}$ plant data	$C_{C,0} = 0$
1	3295	3292
2	939	937
3	354	352
4	213	212
5	180	179
6	172	172

Since the initial carbon loadings are higher than the inherent steady-state carbon loadings of the system, the initial adsorption rates will be low. Hence, output concentrations in the liquid and solid phases will be high initially. Figure 5.11. strongly agrees with this statement.

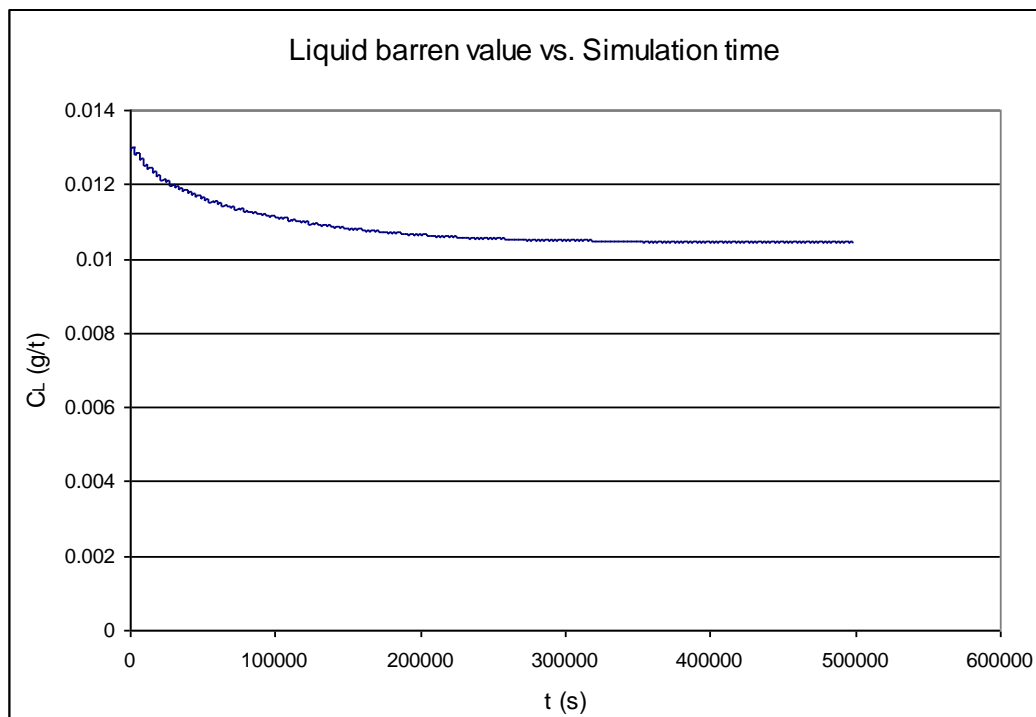


Figure 5.11. : Barren solution gold concentration vs. simulation time (initial loadings specified).

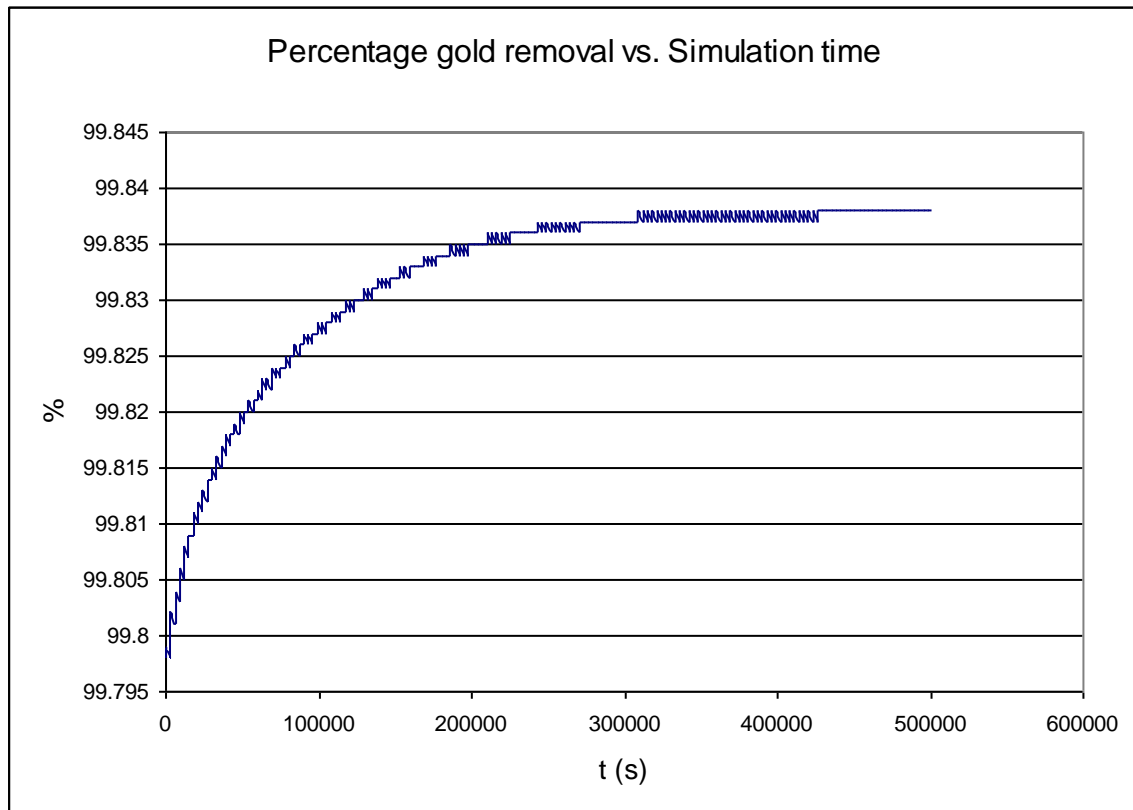
Results for Dynamic CIP Plant Simulation

Figure 5.12. : Overall gold removal percentage (initial loadings specified).

The overall percentage of gold removed compares well for both runs. In both cases a final value of 99.838% is reached. Once again, it can be seen that the system operates uniquely under a given set of operating conditions. The final output concentrations in each stage are independent of initial carbon loading.

Results for Sensitivity Analysis

A Sensitivity Analysis's was performed by varying or creating a step change in each one of the following variables:

- Feed Concentrations (Gold in Solution)
- Feed rate (Solids)
- Elution Efficiency

It was attempted to alleviate the effects of some of these step disturbances by stepping the Fractional Carbon Transfer or Transfer Interval. The effects of these disturbances on process performance were monitored in terms of:

- Barren Solution Concentration
- Loading in first three stages
- Overall Gold Removal

Results for Sensitivity Analysis

6.1. Step-change in Liquid Feed Gold Concentration

At 400 000s, the feed concentration of gold in the liquid phase was stepped from 5.3 to 6.36 g/t (20% increase). Figure 6.1. shows the liquid feed concentration step. Figures 6.2. and 6.3. show the effect on the carbon loading in the first 3 stages and the barren solution concentration respectively.

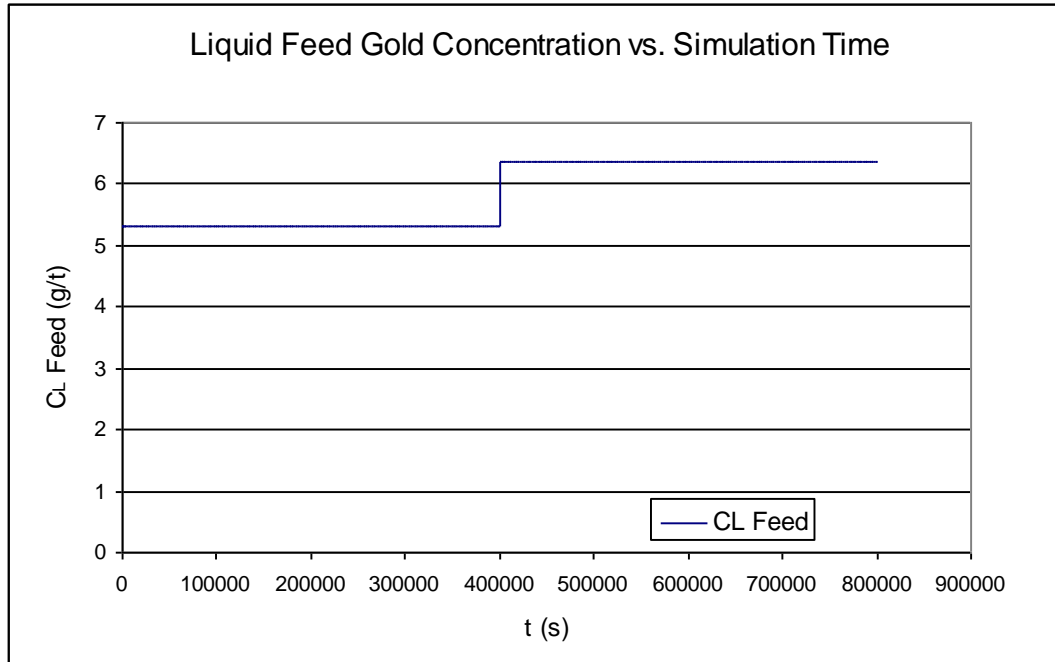


Figure 6.1.: Step in liquid feed gold concentration.

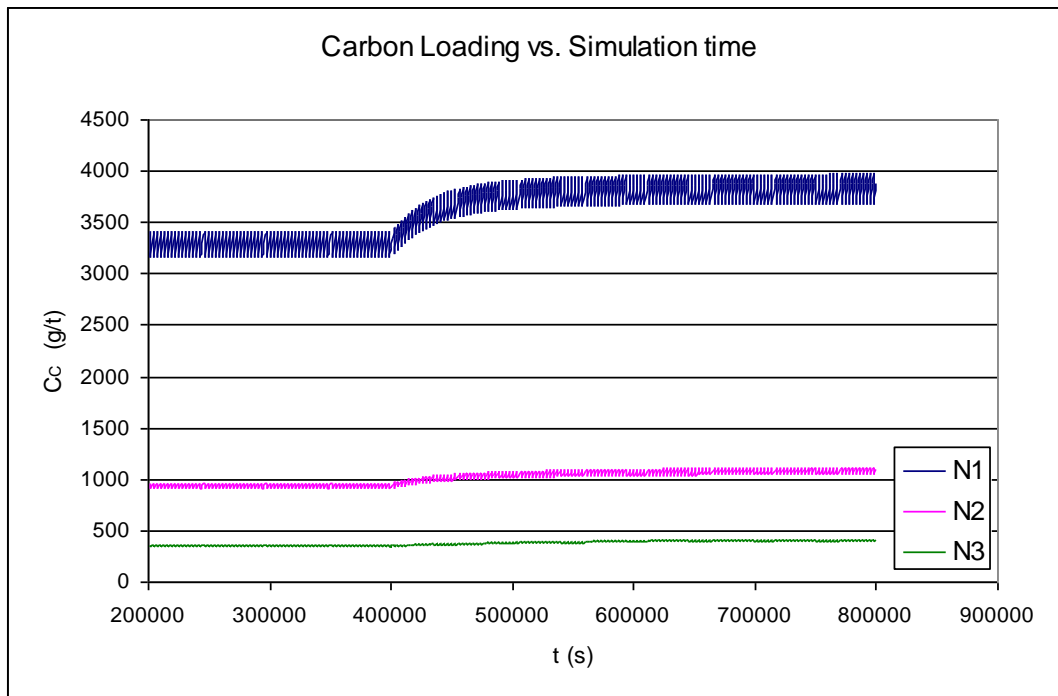
Results for Sensitivity Analysis

Figure 6.2.: Carbon loading profiles (first three stages) resulting from step-change in liquid feed gold concentration.

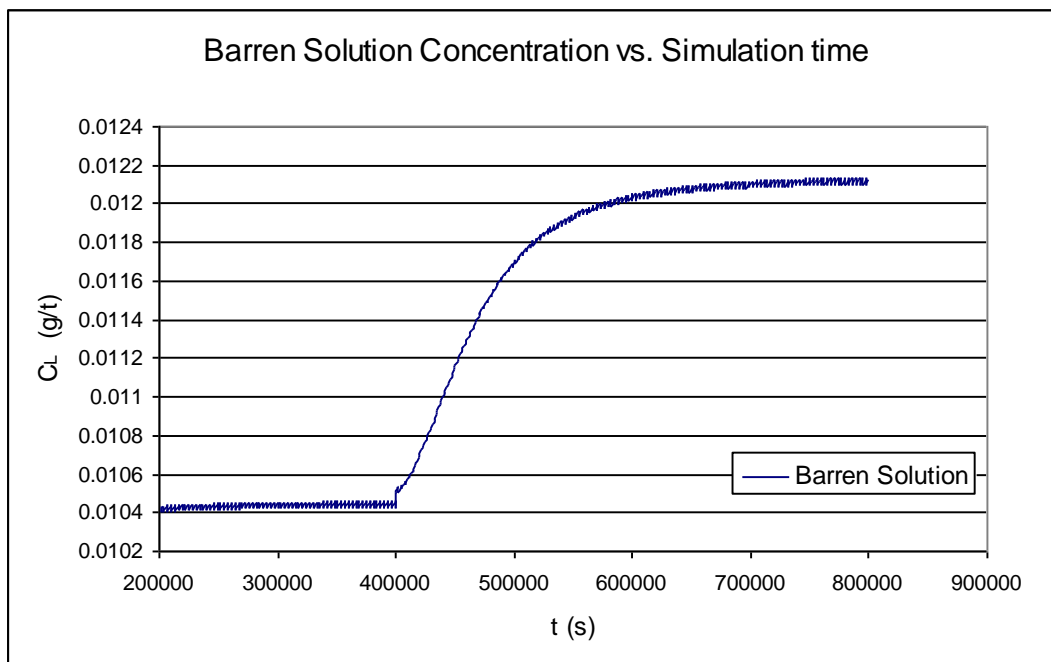


Figure 6.3.: Barren solution concentration profile resulting from step-change in liquid feed gold concentration.

Results for Sensitivity Analysis

Figures 6.2. and 6.3. show how the carbon loading in each stage and the barren solution concentration increase at the moment the step occurs. With the residence time remaining unchanged and the distance from equilibrium increased, it is expected that an increase in the exit liquid phase gold concentrations will occur in every stage. Hence, it would be expected that the barren solution concentration will increase. This is shown by Figure 6.3. The barren solution concentration increases from 0.0104 g/t to 0.0121 g/t.

An increase in solution concentration will result in an increase in adsorption rate in each stage. Thus, higher loadings can be expected in each stage (Figure 6.2.). The carbon loading in the first stage increases from 3411 g/t to 3879 g/t. The simulation once again strives towards a new steady operation.

Results for Sensitivity Analysis

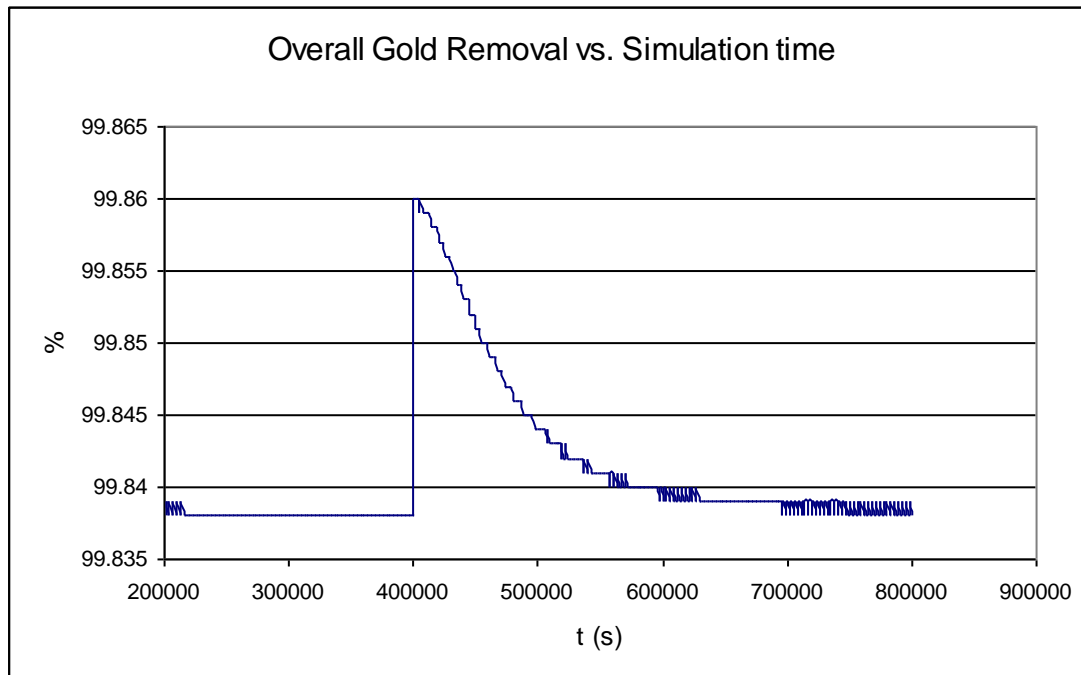


Figure 6.4.: Overall gold removal vs. simulation time resulting from step-change in liquid feed gold concentration.

The overall gold removal only increases at the moment the step occurs, but settles at its initial steady state value once the effect of the step change has propagated through all six stages.

We now attempt to keep the loading in each stage constant by countering the step in liquid feed gold concentration. Stepping either the Carbon transfer fraction or Transfer frequency is investigated as a means of achieving a steady carbon loading in each stage.

Results for Sensitivity Analysis

The Carbon transfer fraction is stepped from 0.1 to 0.115 at 400 000s. This will result in a decrease in average loading in each stage at each transfer interval. Hence, this provides additional loading capacity in each stage.

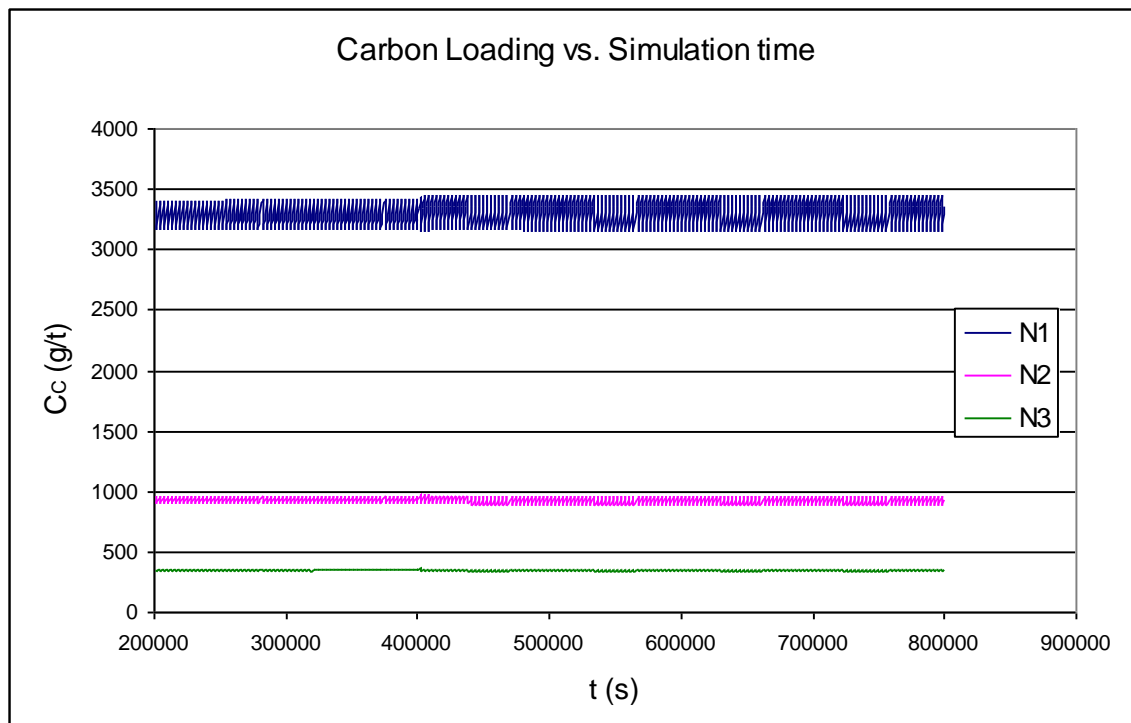


Figure 6.4.: Carbon loading profiles (first three stages) corrected by stepping carbon transfer fraction.

Figure 6.4. shows how the carbon loading profile in the first three stages remain unchanged as a result of an increase in the Carbon transfer fraction. The barren solution concentration changes from 0.0104 g/t to 0.0106 g/t (Figure 6.5.).

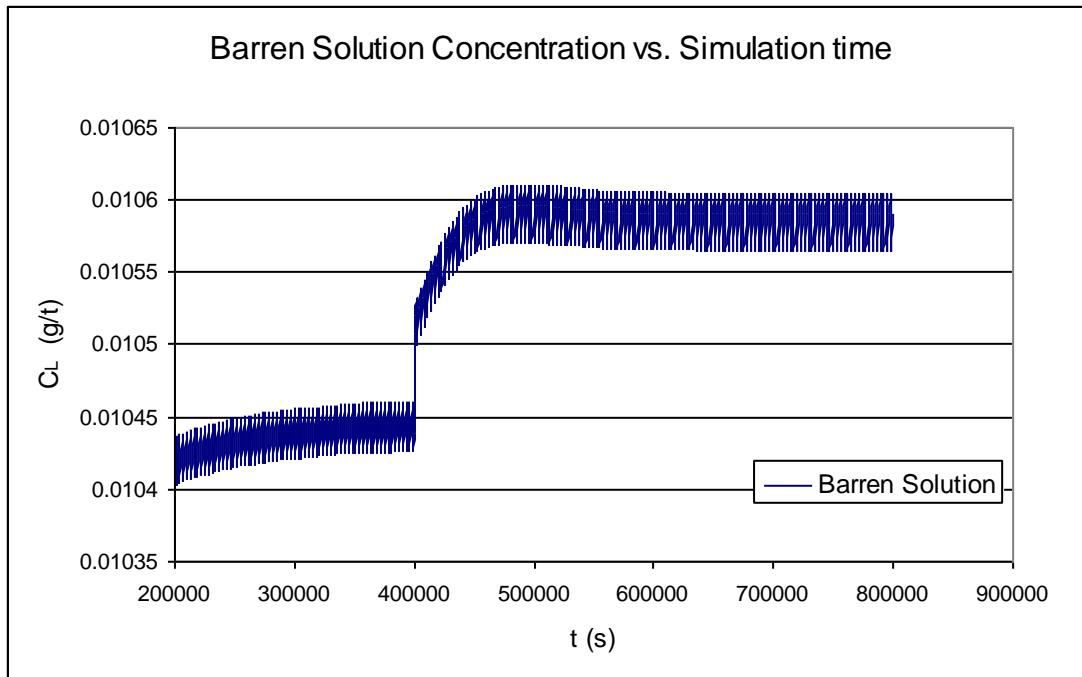
Results for Sensitivity Analysis

Figure 6.5.: Barren solution concentration resulting from a step-change in carbon transfer fraction.

Alternatively, the step in feed solution gold concentration can be countered by stepping the Transfer frequency.

The transfer frequency is stepped down from 3000s to 2570s. This results in the carbon loading profiles illustrated by Figure 6.6.

Results for Sensitivity Analysis

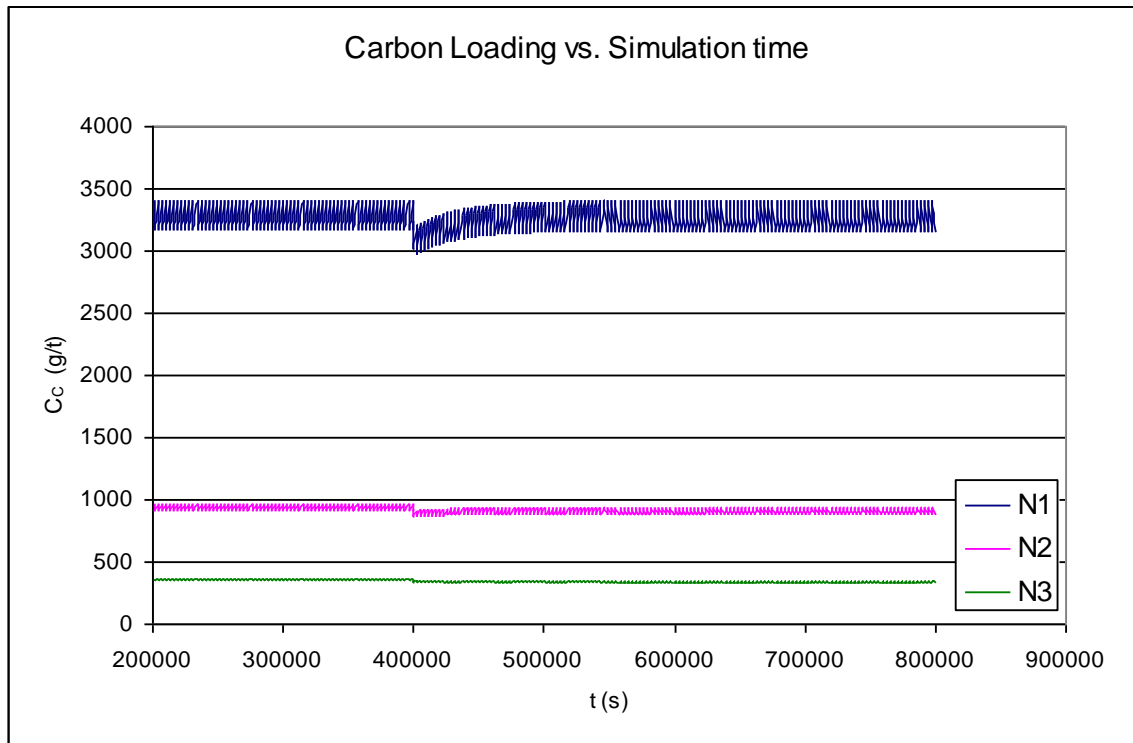


Figure 6.6.: Carbon loading profiles (first three stages) resulting from a step-change in transfer frequency.

Increasing the transfer frequency (decreasing the transfer interval) results in a lower average carbon loading being maintained in each stage over a given time-span. The slight “dip” in the carbon loading profiles that occur at 400 000 s can be ascribed to the delayed effects of adsorption kinetics. Time is needed for the process to acclimatize to the increased transfer frequency. Increasing either the transfer fraction or transfer frequency results in an increase in carbon circulation rate. Hence, the average loading in each stage is decreased. This, in turn, increases the adsorption rate in each stage and so counters an increase in liquid feed gold concentration.

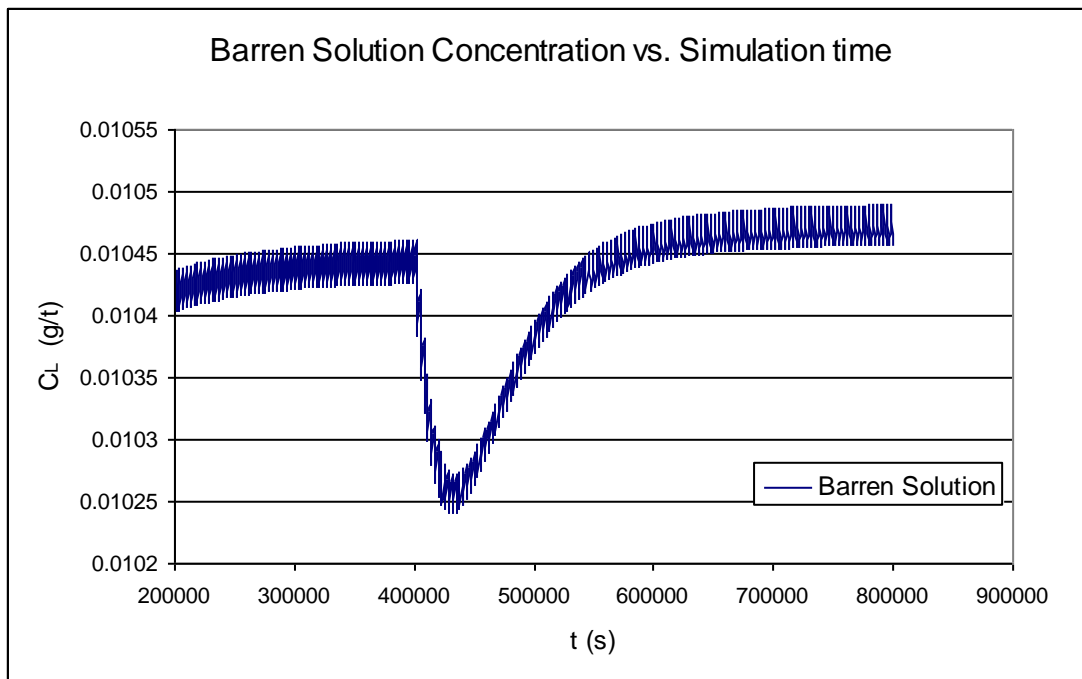
Results for Sensitivity Analysis

Figure 6.7.: Barren solution concentration profile resulting from step-change in transfer frequency.

The barren solution concentration changes from 0.0104 g/t to 0.0105 g/t as a result of stepping the transfer frequency. A sudden decrease in carbon loading occurs in all six stages as a result of a sudden increase in circulation rate. Hence, the slight dip in the barren solution profile is attributed by the delay in adsorption kinetics.

Results for Sensitivity Analysis

6.2. Step-change in Solids Feed Rate

The system is subjected to a 10% increase (from 0.083 t/s to 0.0913 t/s) in solids feed rate at 400 000s.

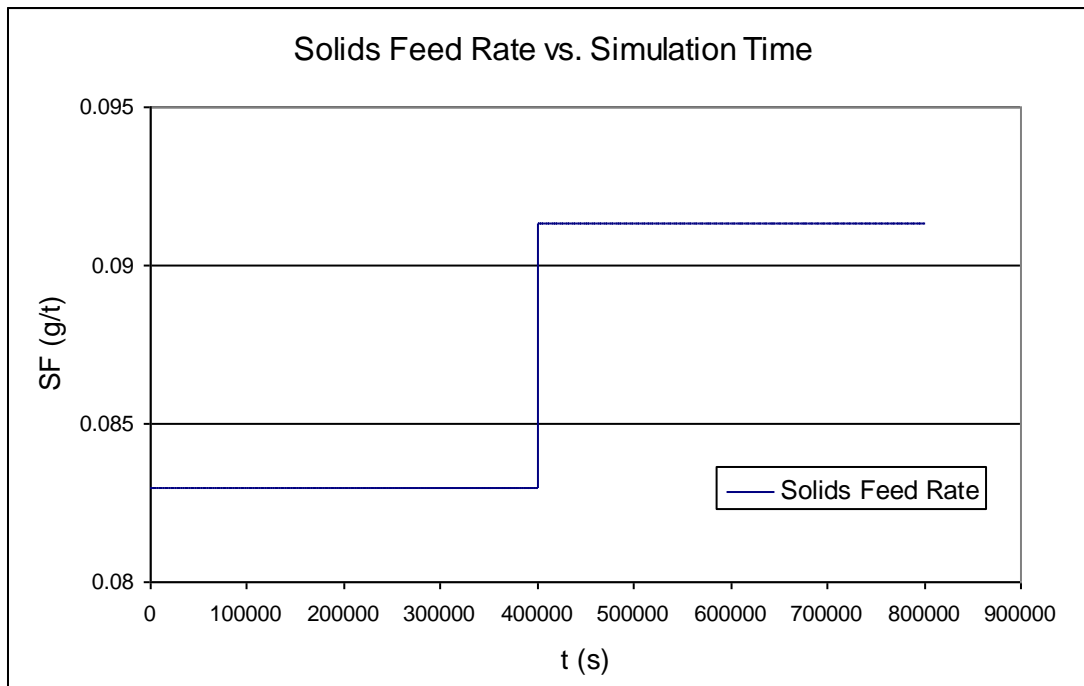


Figure 6.8.: Step-change in solids feed rate.

Results for Sensitivity Analysis

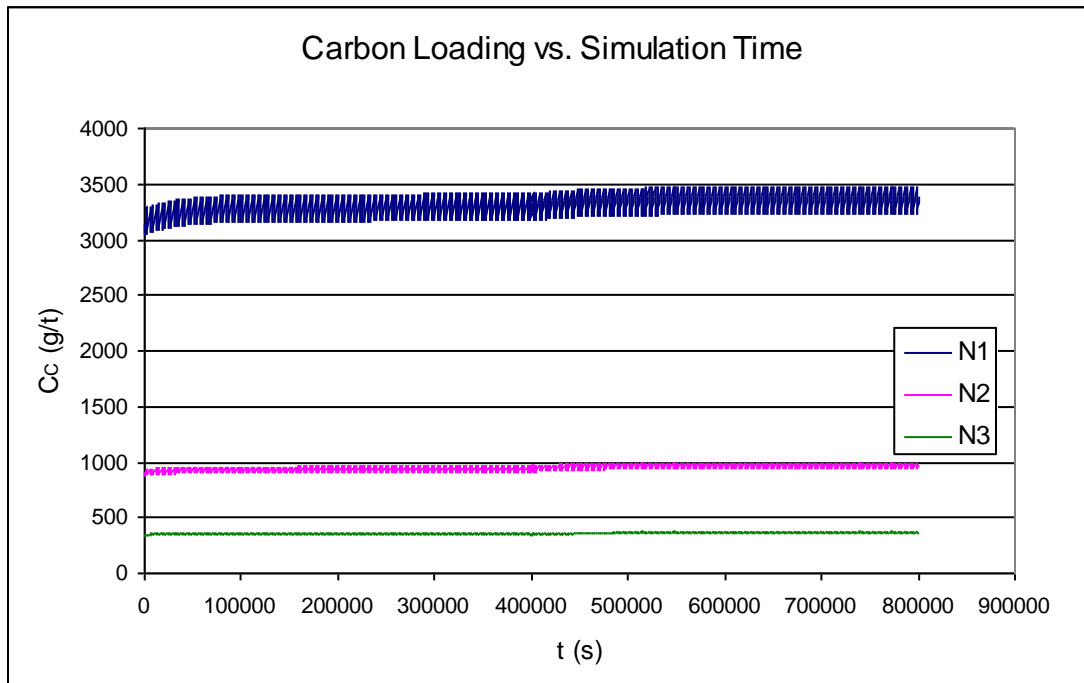


Figure 6.9.: Carbon loading profiles (first 3 stages) resulting from a step-change in solids feed rate.

The carbon loading in the first stage increases from 3280 g/t to 3357 g/t. A step-change in solids feed rate results in an increase in the amount of gold available for leaching and, hence, adsorption in each stage. An increase in feed rate will also result in a decrease in residence time.

A higher carbon loading in each stage, apart from the decrease in residence time, results in a decrease in adsorption kinetics. The empirical rate expression used assumes the rate of adsorption to be proportional to the linear distance from equilibrium (Nicol, 1987). It is therefore expected to see an increase in the barren solution concentration, which is exactly the case. The barren solution

Results for Sensitivity Analysis

concentration changes from a steady value of 0.0103 g/t to a new steady value of 0.0107 g/t after the step-change is initiated.

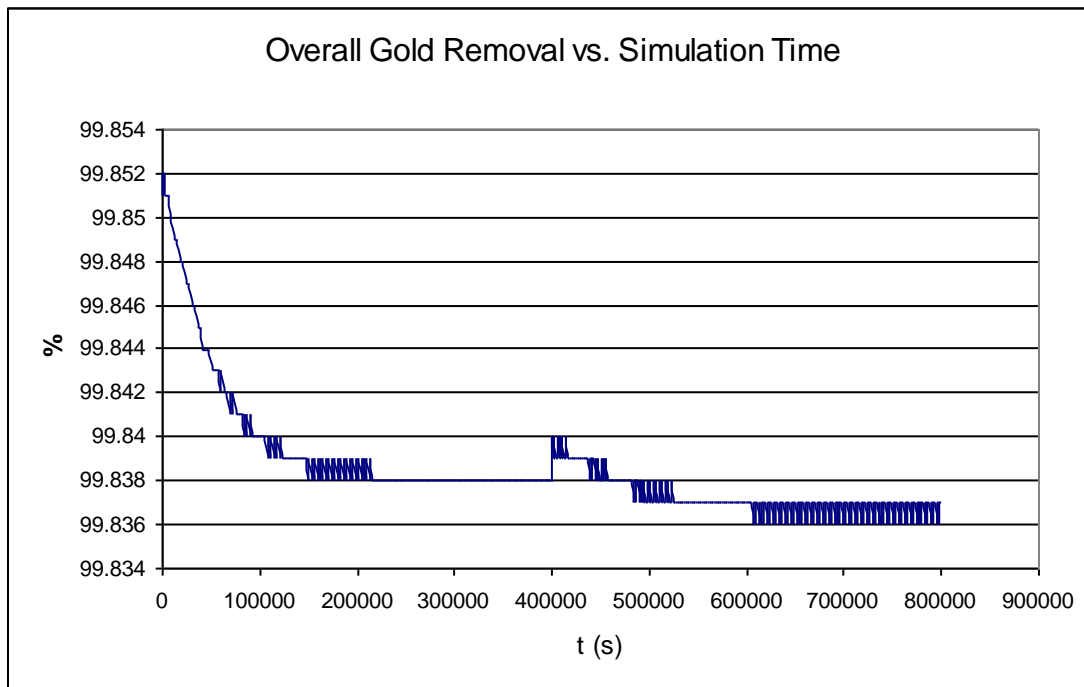


Figure 6.10.: Overall gold removal vs. simulation time resulting from a step-change in solids feed rate.

A decrease in residence time will inevitably lower the overall process efficiency. The shift in carbon loading is ascribed to the increase in gold in the liquid phase, which in turn is the result of increased solid gold feed-rate. With leaching kinetics being rapid in comparison to adsorption kinetics, it is apparent that this shift in operation increases the gold in the liquid phase in each stage. The apparent rise in process efficiency (Figure 6.10.) at 400 000s is due to the sudden increase in gold entering the process. This increase will not be reflected in the barren values immediately.

Results for Sensitivity Analysis

The step-change in solids feed-rate is countered by increasing the fraction of carbon transferred. It is found, by manually increasing the transfer fraction in small increments, that the carbon loadings and barren solution concentration progressively return to their original steady state values. The carbon transfer fraction was increased from 0.1 to 0.120. Alternatively, the optimum step in carbon transfer fraction can be located by programmatic control measures, but it is sufficient here to indicate the direction the simulation takes when this parameter is adjusted.

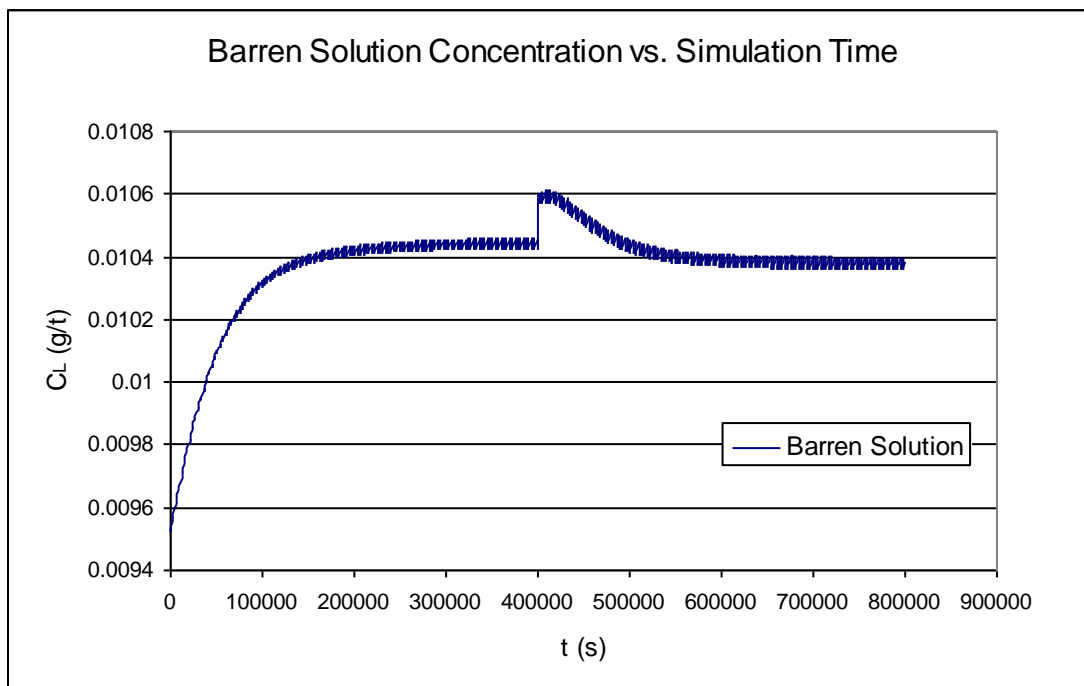


Figure 6.11.: Barren solution concentration profile corrected by step-change in carbon transfer fraction .

Results for Sensitivity Analysis

Figure 6.11. shows the barren solution concentration returning more or less to its original state as a result of increasing the carbon transfer fraction. Similar results may be obtained by decreasing the carbon transfer period. Either way, this will result in a lower average loading per stage after every transfer as both methods causes an increase in carbon circulation-rate (figure 6.12.). Decreasing the average loading results in an increase in adsorption kinetics (Nicol, 1987).

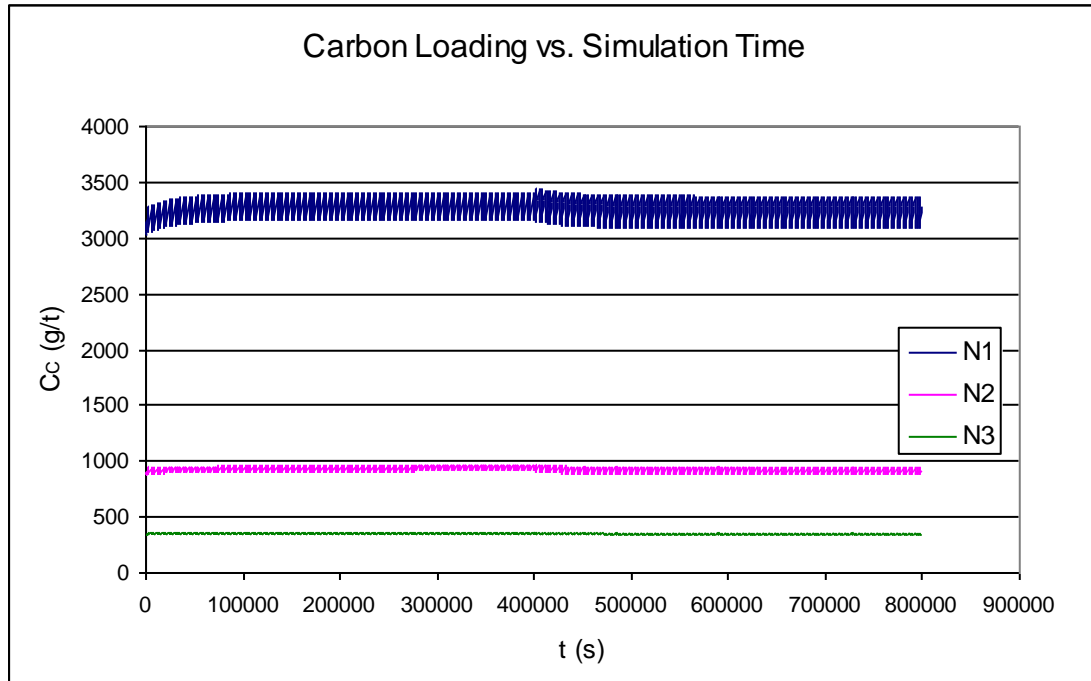


Figure 6.12.: Carbon loading profiles (first 3 stages) corrected by step-change in carbon transfer fraction.

Figure 6.12. shows how the carbon loading profiles in the first three stages continue more or less un-disturbed as a result of the carbon transfer fraction step-change.

Results for Sensitivity Analysis

By decreasing the average loading in each stage, the process's ability to assimilate gold is increased. It is therefore expected to see an increase in process efficiency. This is illustrated by figure 6.13. The overall percentage of gold removed undergoes a rapid increase the moment the carbon transfer fraction is stepped up. Unlike the solids feed-rate step which propagates through the process with a delay, the carbon transfer fraction step is incurred on all six stages simultaneously.

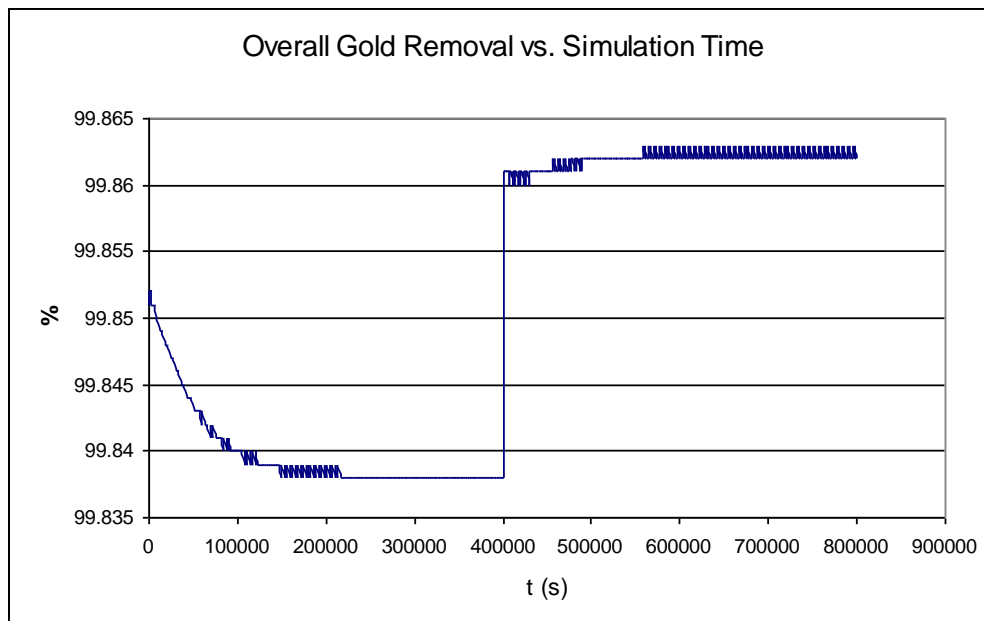


Figure 6.13.: Overall gold removal vs. simulation time resulting from step-change in carbon transfer fraction.

Results for Sensitivity Analysis

6.3. Step-change in Elution Efficiency

The elution efficiency is decreased from 95% to 80% at 400 000s. The simulation time is increased to 1000 000s to allow the process to reach steady loading profiles in each stage.

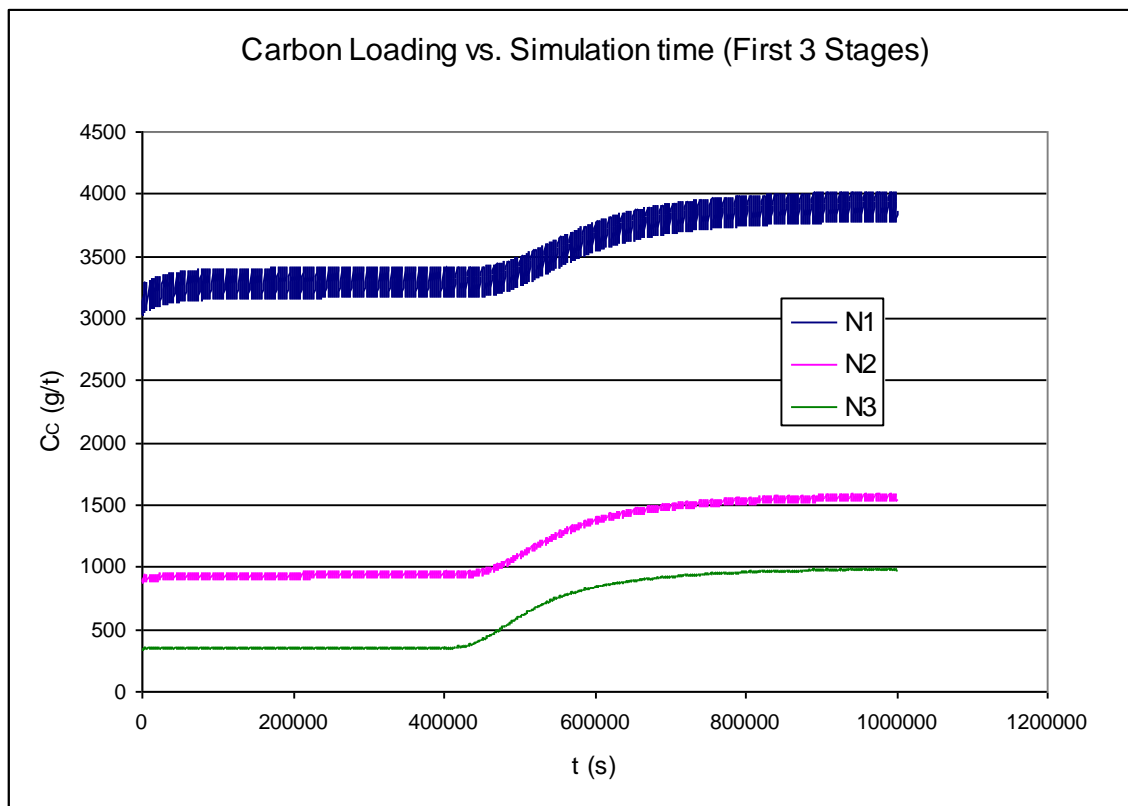


Figure 6.14.: Carbon loading profiles (first 3 stages) resulting from step-change in elution efficiency.

Figures 6.14. and 6.15. depict an increase in carbon loading in every stage. This is a realistic result, since carbon entering the final stage now has a higher loading. Transferring carbon up the train (from N+1 to N) will result in higher

Results for Sensitivity Analysis

average loadings in the preceding stages. Carbon leaving the first stage exhibits an increase in loading from 3280 g/t to 3908 g/t.

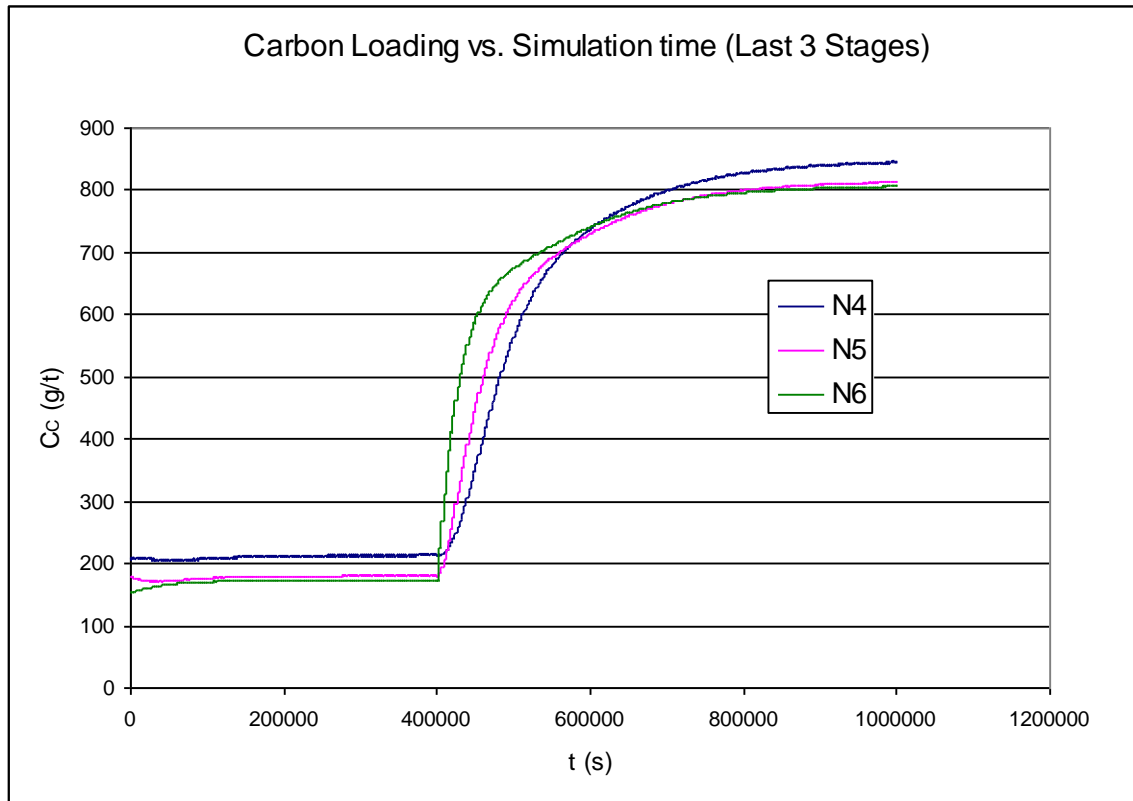


Figure 6.15.: Carbon loading profiles (last 3 stages) resulting from a step-change in elution efficiency.

From figure 6.15. it is notable that the rate of change of loading in the final stage (N6) is greater than that of the preceding stages. The step in elution efficiency will be felt by this stage first. The preceding stages respond relatively slower as they acclimatize to the increase in loading in the final stage. As the step in elution efficiency propagates up the train the loading in the preceding stages progressively increase with every transfer.

Results for Sensitivity Analysis

Figure 6.16. shows an increase in dissolved gold in the effluent from 0.01 g/t to 0.045 g/t. This is a realistic result, since an increase in carbon loading in each stage will certainly have a negative impact on adsorption kinetics.

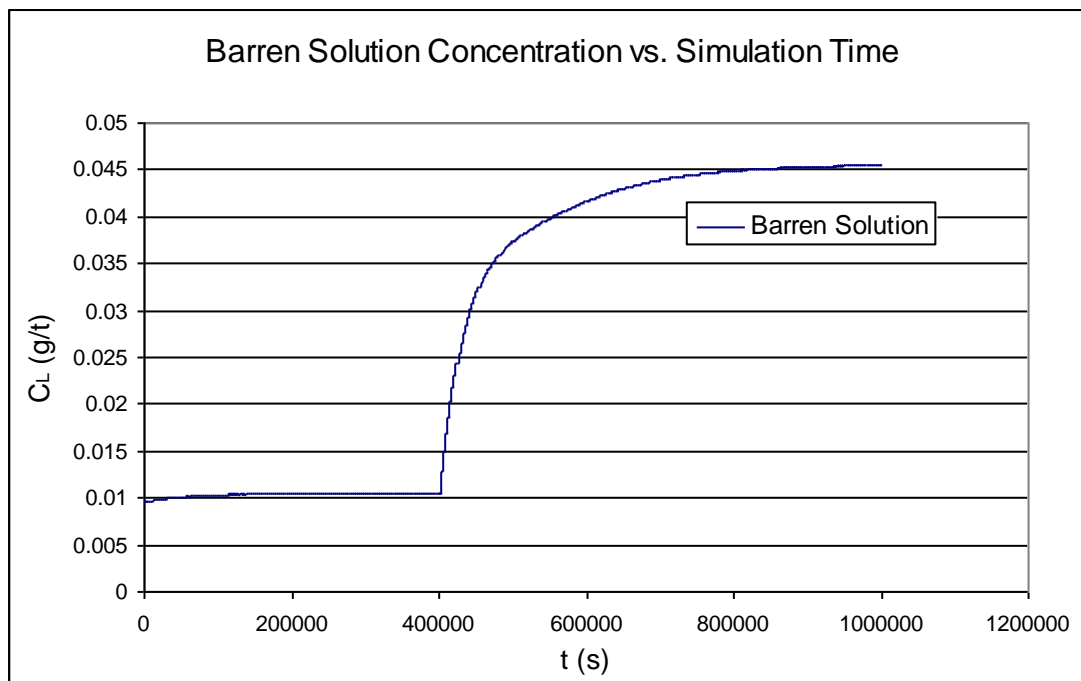


Figure 6.16.: Barren solution concentration profile resulting from a step-change in elution efficiency..

With a 15% drop in elution efficiency, *cet. par.*, it is expected to see a decrease in process efficiency. Figure 6.17. verifies this statement. The overall percentage removed from the gold decreases from 99.84% to 99.29%. It is worth mentioning here that although this decrease is slight, the simulation adequately portrays the direction in which the impinged disturbances affect the process.

Results for Sensitivity Analysis

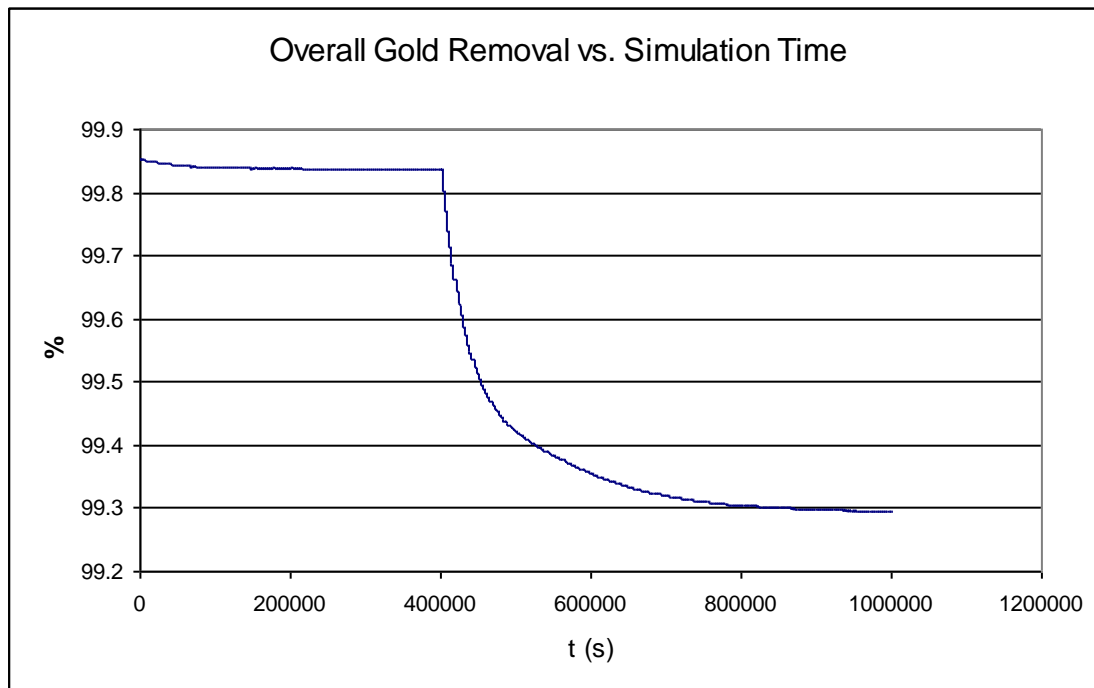


Figure 6.17.: Overall gold removal vs. simulation time resulting from a step-change in elution efficiency.

It was attempted to correct the carbon loading in the first stage by increasing the carbon transfer fraction from 0.1 to 0.118. Figure 6.18. shows the results. The carbon loading in the first stage is brought down to 3291 g/t due to the step in carbon transfer fraction. Figure 6.19. illustrates the comparative results.

It can also be seen from Figure 6.18. that stepping the carbon transfer fraction has less of an impact on the second and third stages. This is reasonable, since transferring carbon up the train results in a cumulative averaging effect that becomes more prominent as the first stage is approached.

Results for Sensitivity Analysis

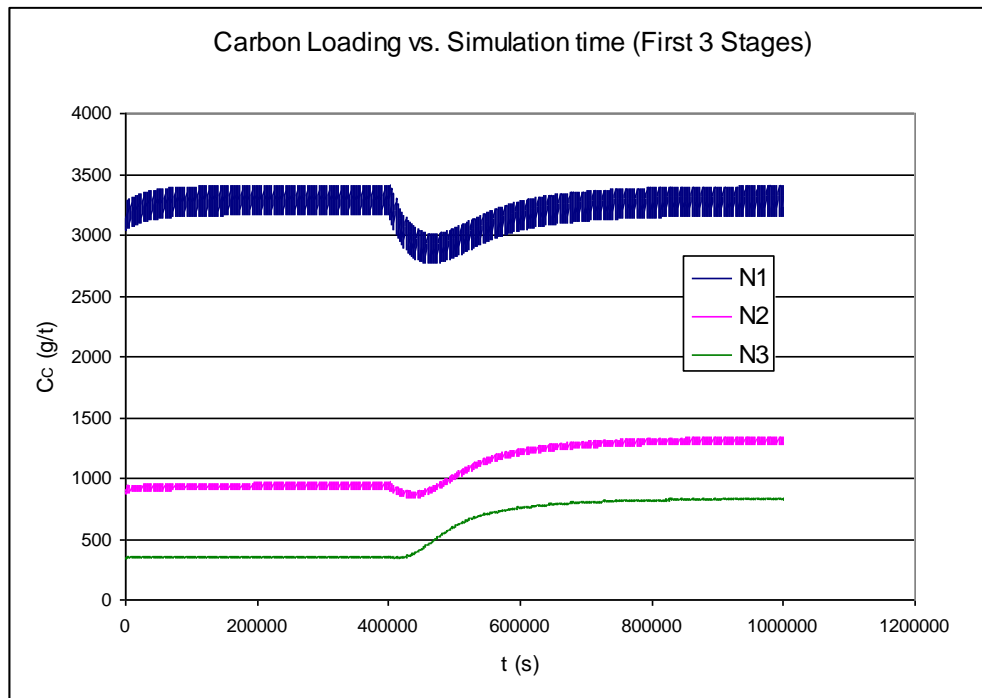


Figure 6.18.: Carbon loading profiles (first 3 stages) resulting from a step-change in carbon transfer fraction.

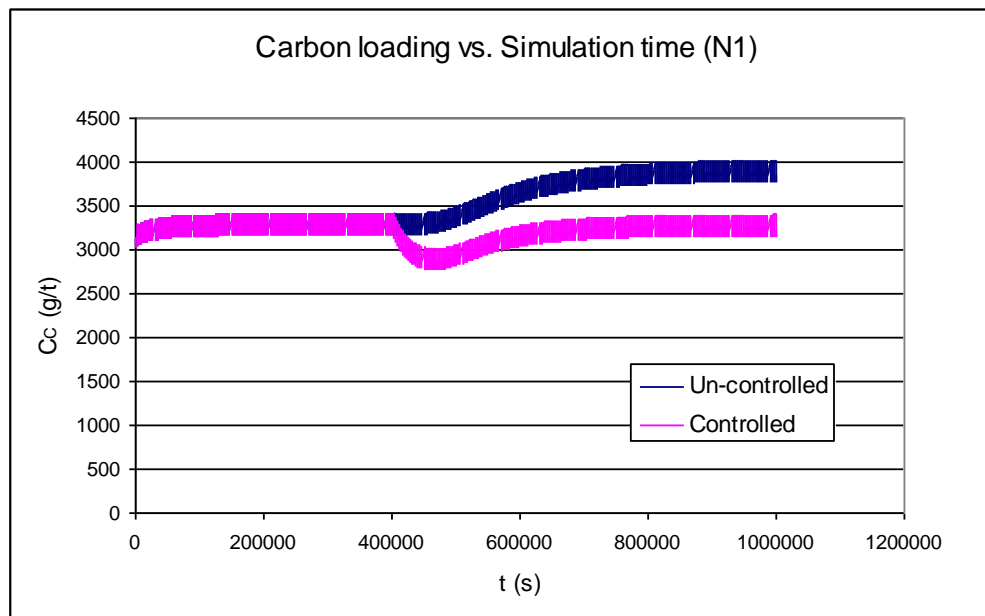


Figure 6.19.: Controlled and un-controlled carbon loading in the first stage.

Results for Sensitivity Analysis

When attempting to keep the dissolved gold in the effluent constant, it was found necessary to increase the fraction of carbon transferred during each transfer interval to 0.43 in order to keep dissolved gold losses at a steady value. Stepping the carbon transfer fraction to 0.43 is very unrealistic. However, it is an indication that the simulation responds as expected. Stepping the carbon transfer fraction has no impact on the loading in the last stage when the elution efficiency is decreased, hence the decrease dissolved gold losses in the effluent can only be attributed to adsorption in the preceding stages.

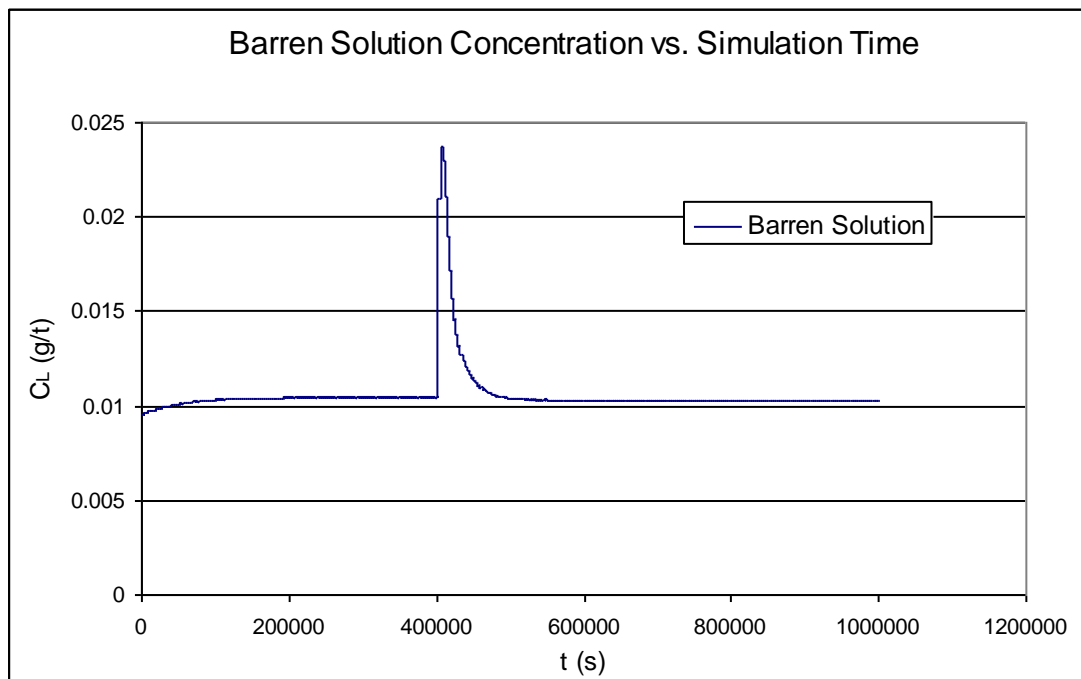


Figure 6.20.: Barren solution concentration profile resulting from a step-change in carbon transfer fraction..

Conclusions

It was shown in this study that simple rate and equilibrium expressions for adsorption and leaching can be used effectively to model CIP/CIL operations when combined with a powerful simulation tool. Matlab Simulink was found to be a suitable simulation tool for dynamic simulations with the disadvantage that a fair level of expertise is required to use this complex software effectively.

Realistic what-if analyses were conducted with the simulation results moving in realistic directions. It was shown how negative effects can be off-set by changing plant operating conditions. This can result in a very powerful tool for plant metallurgists helping to make operation decisions under varying conditions.

Identical carbon loadings in all six stages were reached at steady state, whether initial loadings were specified or not. This indicates that the simulation yields repeatable results under a given set of operating conditions.

Sensitivity analyses qualitatively and quantitatively reflect the effects of disturbances imposed on the system. In each case the process simulation yielded realistic results. It was possible, in turn, to counter these disturbances by manipulating another plant parameter.

Conclusions

A chronological solution, which may be used by plant personnel, was developed. Such a tool may assist plant engineers to achieve optimum efficiency and investigate better control strategies.

Bibliography

Bailey, P.R. 1987. Application of Activated Carbon to Gold Recovery. In Stanley, G.G. (ed.). *The Extractive Metallurgy of Gold in South Africa. Volume 1. Johannesburg: The South African Institute of Mining and Metallurgy.*

Coulson, J.M., Richardson, J.F., Bachhurst, J.R. and Harker, J.H. 1999. *Chemical Engineering Volume 1. 6th ed.* Oxford: Butterworth-Heinemann

Coulson, J.M., Richardson, J.F., Bachhurst, J.R. and Harker, J.H. 1999. *Chemical Engineering Volume 2. 4th ed.* Oxford: Butterworth-Heinemann

Flemming, C.A. and Nicol, M.J. 1981. The kinetics of gold adsorption onto activated carbon from cyanide pulp. *Mintek Confidential Communication*. No C620.

Kudryk, V. and Kellog, H.H. 1954. Mechanism and rate controlling factors in the dissolution of gold in cyanide solution, *J.Met., Trans, AIME*, 6(5):541-548

Laxen, P.A. 1984. Carbon-in-pulp processes in South Africa. *Hydrometallurgy*, 13(1984):169-192.

Matlab, *The Mathworks, Inc.*, 2004

Mintek. 2004.

<http://www.mintek.co.za/EMD/CIP/cip.htm>

[25 June 2004]

Nicol, M.J., Fleming, C.A. and Cromberge, G. 1984. The adsorption of gold cyanide onto activated carbon. *Johannesburg: South African Institute of Mining and Metallurgy*, 84(2),50-54.

Schubert, J.H., Barker, I.J. and Swartz, C.L.E. 1993. Performance Evaluation of a carbon-in-pulp plant by Dynamic Simulation. *Johannesburg: South African Institute of Mining and Metallurgy*, 93(11-12), 293-299.

Stange, W. 1991. The optimization of the CIP Process using mathematical and economic models. *Minerals Engineering*, 4(12):1279-1295.

Van Deventer, J.S.J. and Ross, V.E., The dynamic simulation of carbon-in-pulp systems: A review of recent developments. *Minerals Engineering*, 1991, 4(7), 667-681.

Paper published

APPENDIX A
